1971

Experimental Investigation of Shock Boundary Layer Interaction for Two-Dimensional and Axisymmetric Flow

A. Shawki Zahran

EXPERIMENTAL INVESTIGATION OF SHOCK BOUNDARY LAYER INTERACTION FOR TWO-DIMENSIONAL AND AXISYMMETRIC FLOW

BY

A. SHAWKI ZAHRAN

A thesis submitted
in partial fulfillment of the requirements for the
degree Master of Science, Department of
Mechanical Engineering, South
Dakota State University

1971

EXPERIMENTAL INVESTIGATION OF SHOCK
BOUNDARY LAYER INTERACTION FOR
TWO-DIMENSIONAL AND AXISYMMETRIC FLOW

This thesis is approved as a creditable and independent investigation by a candidate for the degree, Master of Science, and is acceptable as meeting the thesis requirements for this degree, but without implying that the conclusions reached by the candidate are necessarily the conclusions of the major department.

_____ _____

Thesis Adviser Date

_____ _____

Head, Mechanical Engineering Department Date

ACKNOWLEDGMENT

The author is indebted to Dr. Edward Lumsdaine for his initiation, guidance and counceling which led to the work presented here.

The author also wishes to thank the Mechanical Engineering Department, South Dakota State University and the National Science Foundation for supporting this work under Grant No. GK 5030 awarded to Dr. Lumsdaine.

TABLE OF CONTENTS

LIST OF FIGURES

CHAPTER I

INTRODUCTION

A supersonic wind-tunnel has been constructed using an 8 inch by 10 inch single stage jet vacuum ejector with a capacity of handling 0.4 lb/sec air at 4 inches Hg absolute suction pressure. A Toepler Schlieren system with 10-inch diameter parabolic mirrors has been set up for flow pattern visualization. The same apparatus was developed to obtain multi-colored views of the flow pattern. That was accomplished by placing an equilateral prism in front of the light source located at the focal plane of the first parabolic mirror. A spectrum was thus produced at the focal plane of the second parabolic mirror, and the color of the image on the screen could be adjusted by moving a slit (parallel to the bands of the spectrum) across the spectrum.

An optical method was developed for visualization of the flow over axisymmetric bodies. A special cylindrical lens test section was designed such that a parallel beam of light coming to one side of the lens would be refracted parallel through its circular cavity and then refracted out parallel on the other side.

Using the supersonic tunnel, experiments were conducted on shock boundary layer interaction at low Mach numbers (about 1.3) with two-dimensional as well as axisymmetric models. For the same area ratio the two-dimensional model showed severe flow separation from one side but the axisymmetric model showed little or no flow separation both from the pressure data and the optical data. By inserting a plate horizontally, thus dividing the two-dimensional test section into two halves, the severe flow separation was almost eliminated. Although the shock wave is clearly visible when using the optical method for axisymmetric flow, minor flow separation could not be detected using this technique.

Theoretical solutions to turbulent incompressible boundary layers for flow over axisymmetric or two-dimensional bodies are well known /1/*. Although these methods area fairly accurate for determining boundary layer growth, the accuracy deteriorates rapidly near the separation point. For the case of compressible flow, the situation is even worse. Thus experimental investigations of compressible boundary layers are needed. A detailed

---

*Numbers in brackets refer to references at the end of the text.

theoretical discussion of compressible boundary layers and shock boundary layer interaction for flow in an axisymmetric inlet is given in Reference 2.

The construction of the supersonic tunnel described in this thesis and the testing of several two-dimensional as well as axisymmetric models using this tunnel were made to provide a facility where experimental tests can be conducted on various aspects of flow separation and shock boundary layer interaction.

CHAPTER II

APPARATUS

A. Wind Tunnel Airflow Path

1. An 8 inch by 10 inch steam jet ejector is used for sucking the atmospheric air through the test section (Figure 1). This steam jet ejector uses about 10,000 lb/hr of steam at about 75 psig pressure. Figure 2 shows the performance curve of this ejector. To get the required pressure drop across the test section, a diffuser is built in between the exit of the test section and the suction flange of the ejector. A silencer is also installed at the exhaust end of the ejector. A photograph of the complete installation is shown in Figure 3.

2. A multitube mercury manometer (36 tubes) is used to messure the static and total pressure distributions in the test section. A single tube manometer measures the suction pressure of the steam ejector to determine the main air flow through the test section, using the performance curve of Figure 2. The steam pressure is adjusted to the indicated value of 75 psig.

3. The secondary air for tangential blowing is provided from a two-cylinder reciprocating compressor

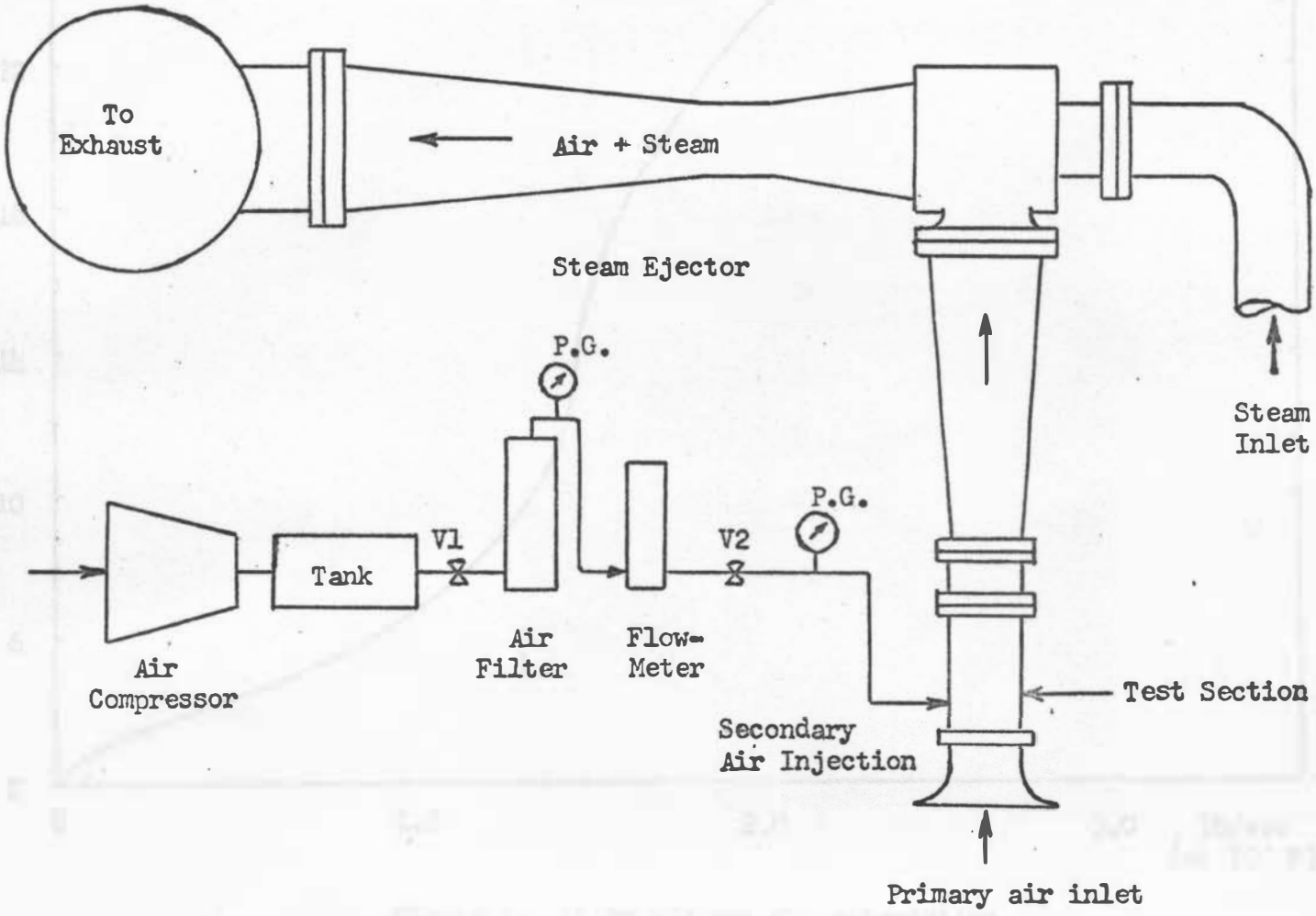

Figure 1. Schematic of the wind tunnel (without Schlieren).

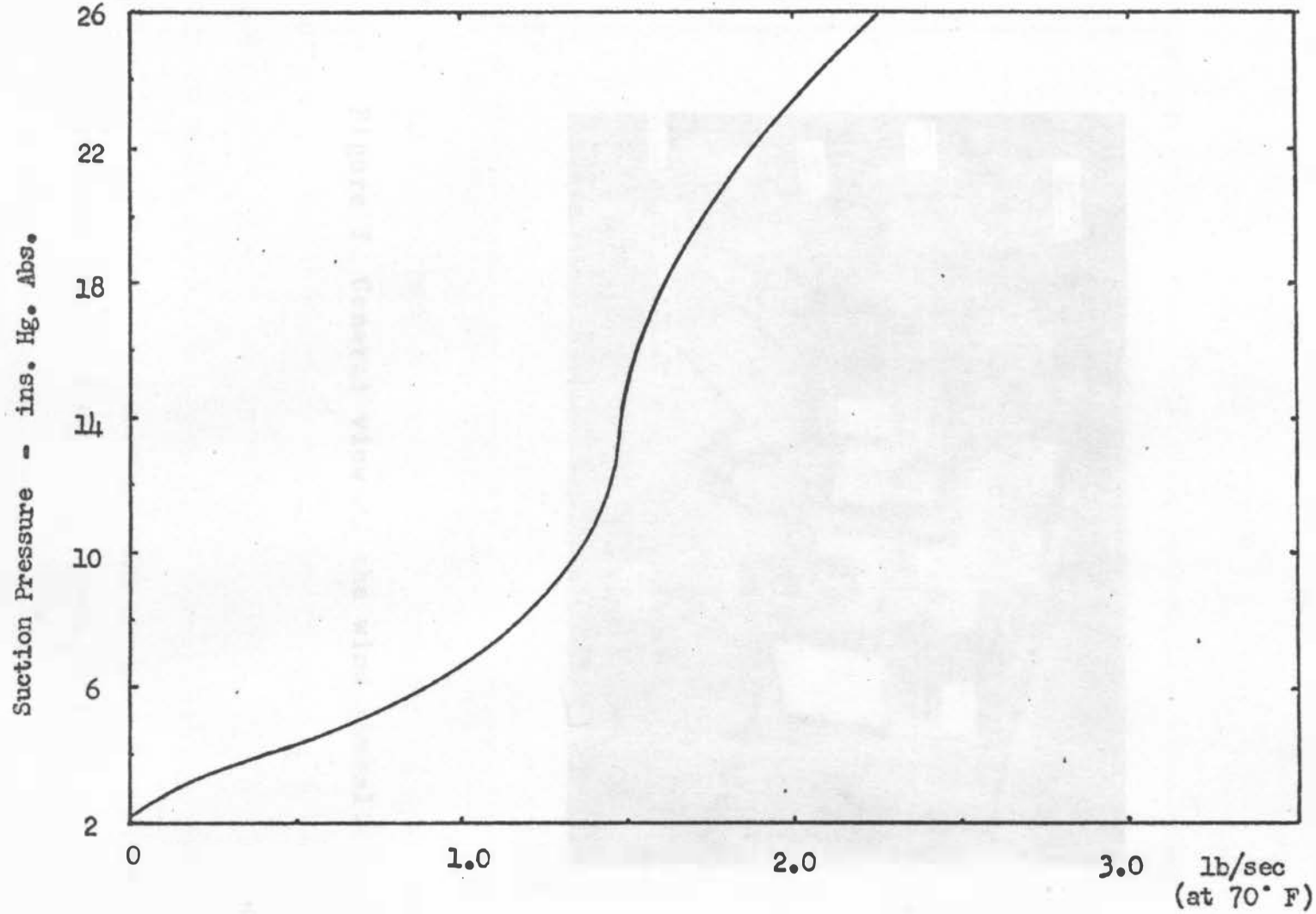

Figure 2. Steam ejector characteristics.

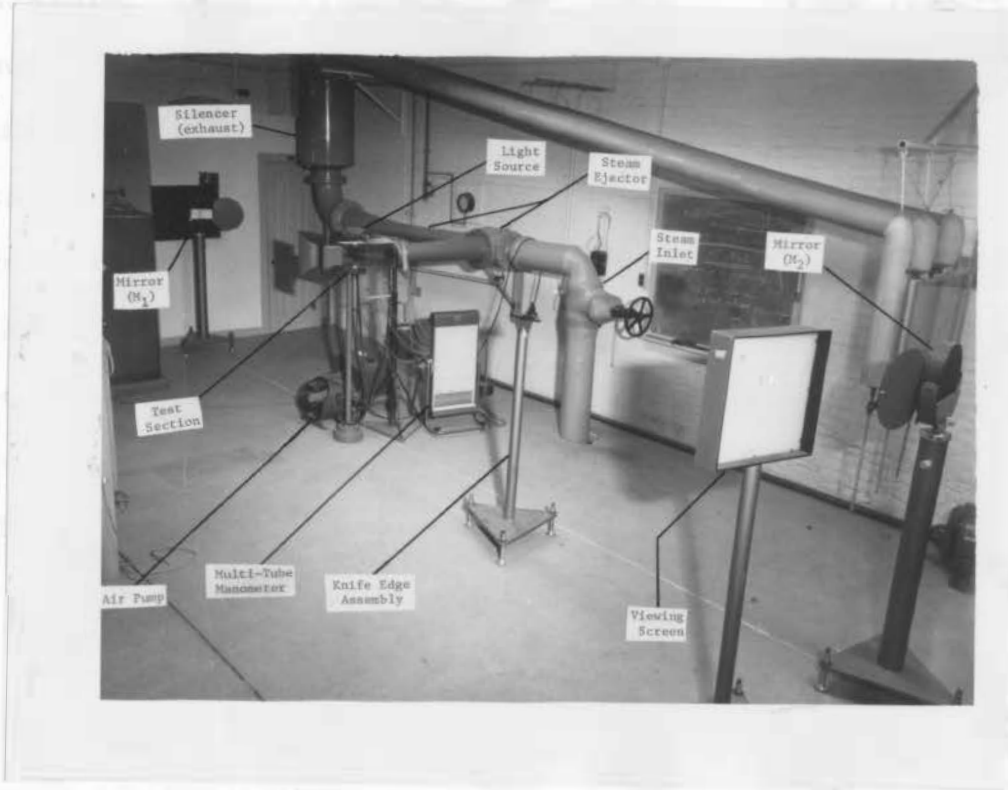

Figure 3. General view of the wind tunnel.

to a collecting tank through a cartridge type air filter which is capable of filtering any dirt as well as oil and water condensate. A rotary-type flow meter is also used to measure the airflow just before it is blown into the test section (Figure 1). A primary control valve (V1) is installed preceding the air filter, while the air flow to be blown into the test section is regulated by a second gate valve (V2) which is located after the flow meter. The inlet air pressure to the flow meter is measured to monitor the air flow. Another pressure gauge is also used to measure the blowing air stagnation pressure just before the air enters the test section.

B. Visualization of the Flow Pattern

Flow pattern visualization is a very useful technique in high-speed aerodynamic research to help with the pressure measurements for better analysis of the test results. Many optical methods are known [3] which depend on the density change or the density gradient in the flow path which affect the refractive index. The most practical method used is the Toepler Schlieren system because it depends mainly on the density gradient in the flow path rather than on the change in density. A basic Schlieren

system was first constructed for this investigation and was then further developed from black and white views to colored ones. The black and white system is presented first, followed by a description of the improved colored Schlieren system.

1. Black and White Schlieren System:

The layout of such a system is shown in Figure 4. The light source S is a high pressure mercury arc lamp which requires a D.C. power supply with a high initial voltage for starting, and a variable resistor to adjust the current. Two parabolic mirrors, M1 and M2, with an 80-inch focal length, are adjusted to get a parallel beam of light through the test section.

At the focal plane of the second mirror M_2, where an image of the light source is formed, a knife edge K (or a graded filter) is located. The knife edge has a horizontal and a vertical edge in a right angle assembly which can be adjusted in the vertical as well as the horizontal directions. The light beam is then received by the plain mirror M_3 which in turn reflects it to the viewing screen.

All components are set up properly when the introduction of the knife edge to cut the image in either

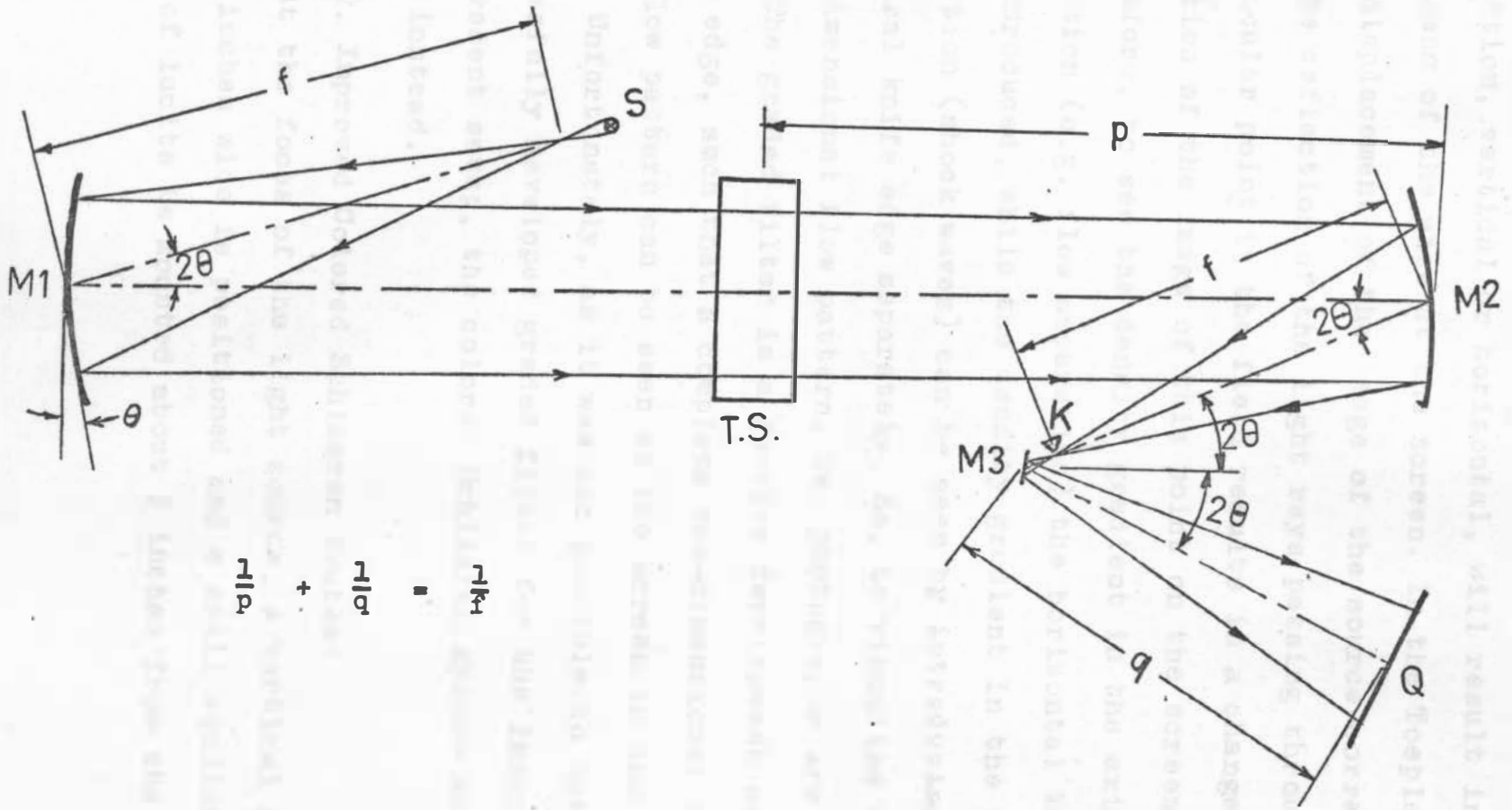

$$\frac{1}{p} + \frac{1}{q} = \frac{1}{f}$$

Figure 4. Layout of the optical system for black and white Schlieren.

direction, vertical or horizontal, will result in uniform darkness of the view at the screen. In the Toepler method the displacement of the image of the source corresponding to the deflection of the light rays passing through a particular point in the field results in a change of illumination of the image of this point on the screen [4]. Therefore, to see the density gradient in the axial direction (e.g. flow separation) the horizontal knife edge is introduced, while the density gradient in the vertical direction (shock waves) can be seen by introducing the vertical knife edge separately. So, to visualize a complete two-dimensional flow pattern, two photographs are required.

The graded filter is a further development of the knife edge, such that a complete two-dimensional view of the flow pattern can be seen at the screen in one adjustment. Unfortunately, as it was not possible to obtain a successfully developed graded filter for the image size in the present setup, the colored Schlieren system was developed instead.

2. Improved Colored Schlieren System:

At the focus of the light source, a vertical slit (S1) 0.060 inches wide is positioned and a small equilateral prism of lucite is mounted about 3 inches from the slit (S1).

The mounting of the prism allows some linear adjustments along the light path as well as angular adjustments to give a full spectrum from red to blue across the first mirror M_1. Instead of the knife edge, another vertical slit (S2) is employed whose width is equal to about one half of the light source image and whose height is slightly smaller than the full height of the image. With this arrangement (Figure 5), a complete two-dimensional colored view of the flow pattern is obtained at the screen Q. Since colored reproductions are very expensive, Figure 6 is given in black and white. The colored negative or prints are available in the Mechanical Engineering Department.

C. Practical Considerations

1. Effects of Diffraction:

It is found that, although the illumination on the viewing screen is usually approximately constant in the absence of the knife edge, this is no longer the case when a knife edge is present. The effects of diffraction then usually result in increased illumination on the viewing screen. Also, the illumination does not fall sharply to zero at the boundaries but dies away gradually.

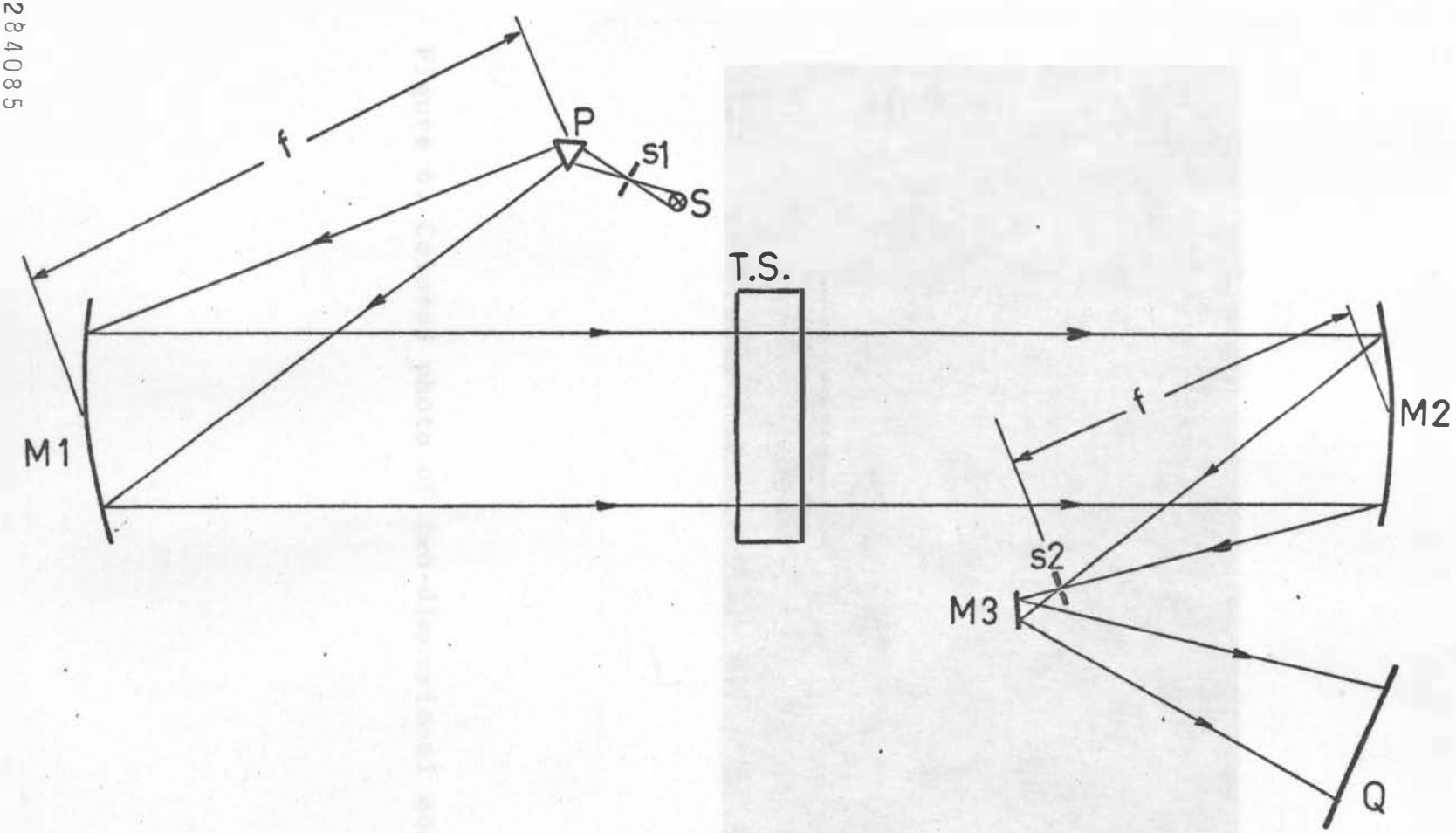

Figure 5. Layout of the developed colored Schlieren system

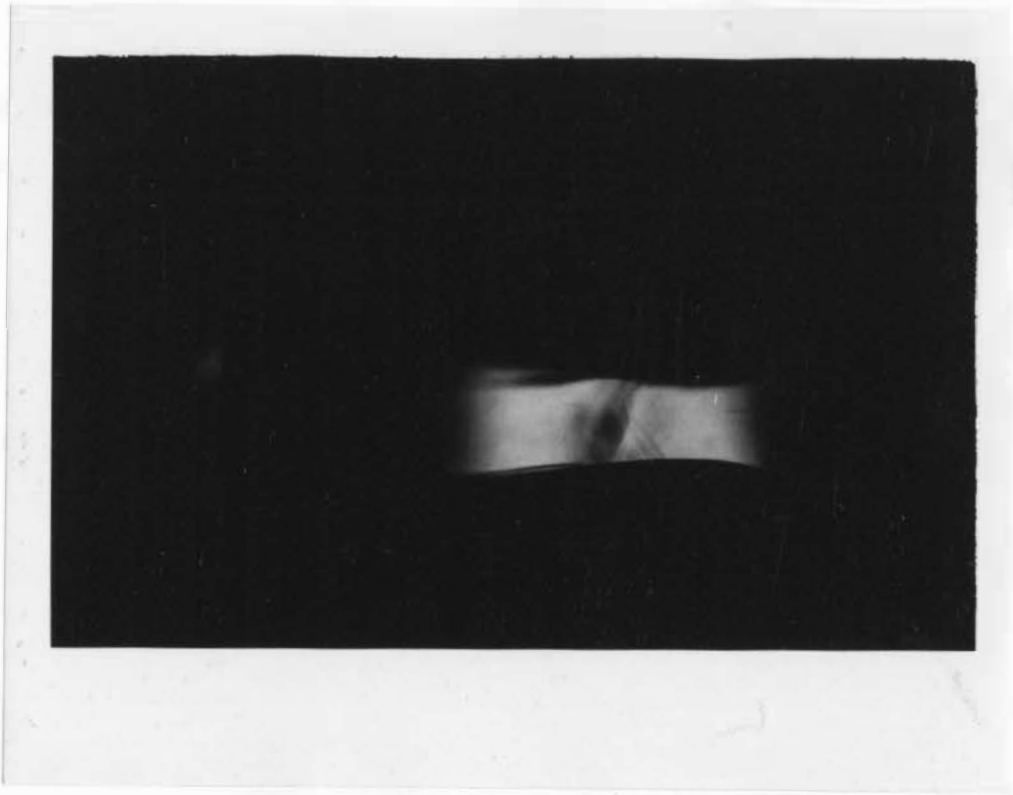

Figure 6. Colored photo of two-dimensional model.

The magnitude and extent of these effects increase as the proportion of the image of the source cut off by the knife edge is increased /3/.

2. Location of Light Source:

The angles between the mirror axis and the light source or the knife edge assembly should be twice the angle of the parabolic mirrors. An off-axis mirror system causes uneven illumination on the screen, even when no optical disturbance is present. To reduce these effects, the light source and the knife edge should be located on opposite sides of the mirror axes.

CHAPTER III

DESCRIPTION OF TEST MODELS

A. Two-Dimensional Flow

Three profiles were constructed to investigate the effect of the upstream velocity profile on the shock boundary-layer interaction. They have exactly the same profile for the divergent section downstream of the throat. The two-dimensional model is formed by two blocks of hard wood profiled as shown in Figure 7 and screwed onto the sides of two optically clear 0.50-inch thick plexiglass plates. The two blocks of wood were shaped together in one pattern, separated, and then very symmetrically located between the plexiglass plates (which are 4.0 inches apart) to give a throat area for profiles I,II and III of 1.333 x 4.0 square inches. Profile A is similar to profile I but with a throat area of 1.00 x 4.00 square inches.

All test sections were installed with the plexiglass plates exactly normal to the parallel light beam of the Schlieren system. A two-dimensional bell mouth was fabricated to fit these two-dimensional models. Static

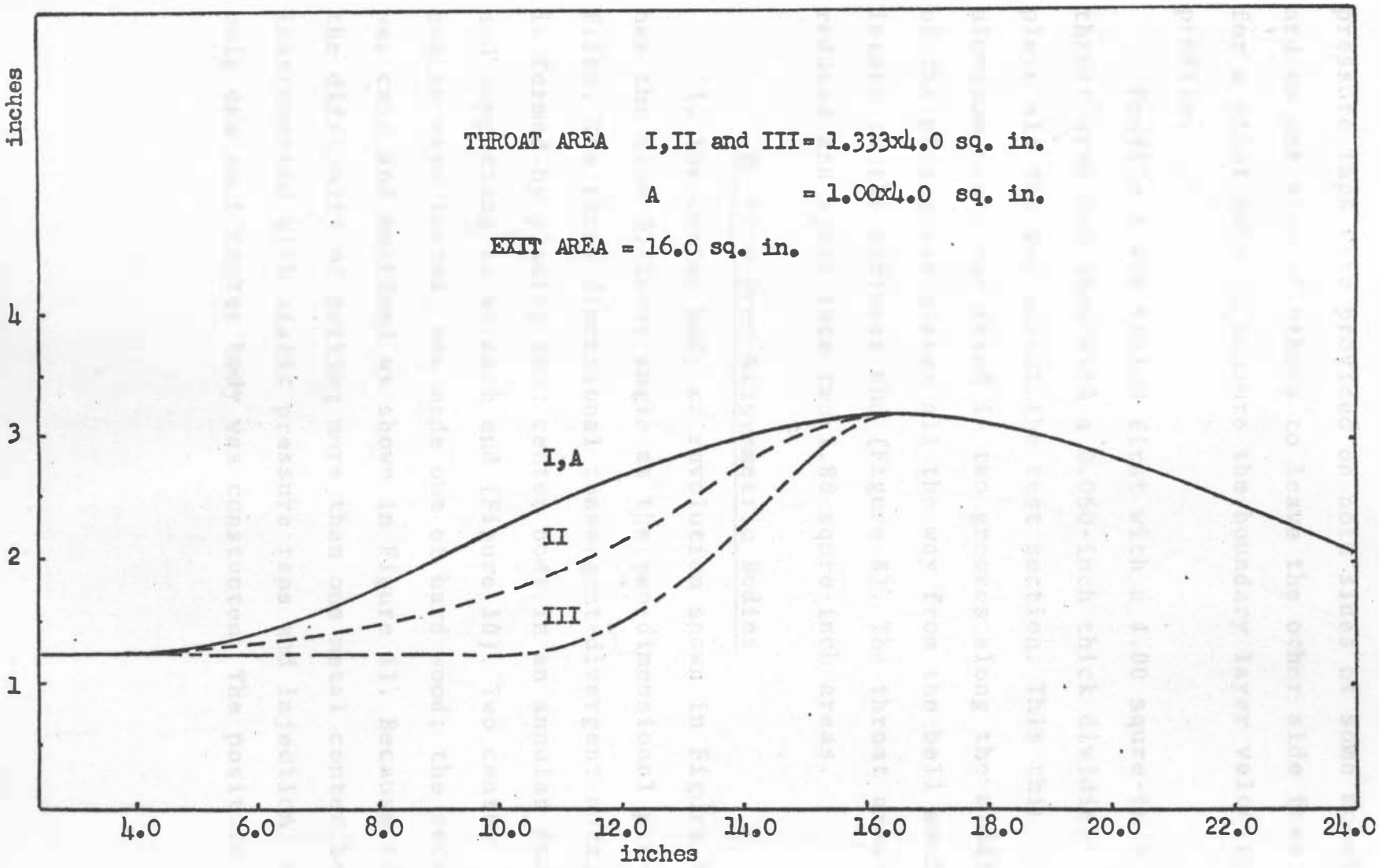

Figure 7. Two-dimensional profiles of models A, I, II and III.

pressure taps were provided on both sides of some models and on one side of others to leave the other side free for a pitot tube to measure the boundary layer velocity profile.

Profile A was tested first with a 4.00 squre-inch throat area and then with a 0.060-inch thick dividing plate all the way across the test section. This thin aluminum plate was fixed in two grooves along the middle of the plexiglass plates all the way from the bell mouth intake to the diffuser end (Figure 8). The throat area was reduced and split into two 1.88 squre-inch areas.

B. Flow Over Axisymmetric Bodies

1. The center body of revolution shown in Figure 9 has the same diffuser angle as the two-dimensional profiles. The three-dimensional convergent-divergent nozzle is formed by placing that center body in an annular duct and supporting it at each end (Figure 10). Two center bodies were tested, one made out of hard wood; the second was cast and machined as shown in Figure 11. Because of the difficulty of getting more than one metal center body instrumented with static pressure taps and injection slots, only one such center body was constucted. The position

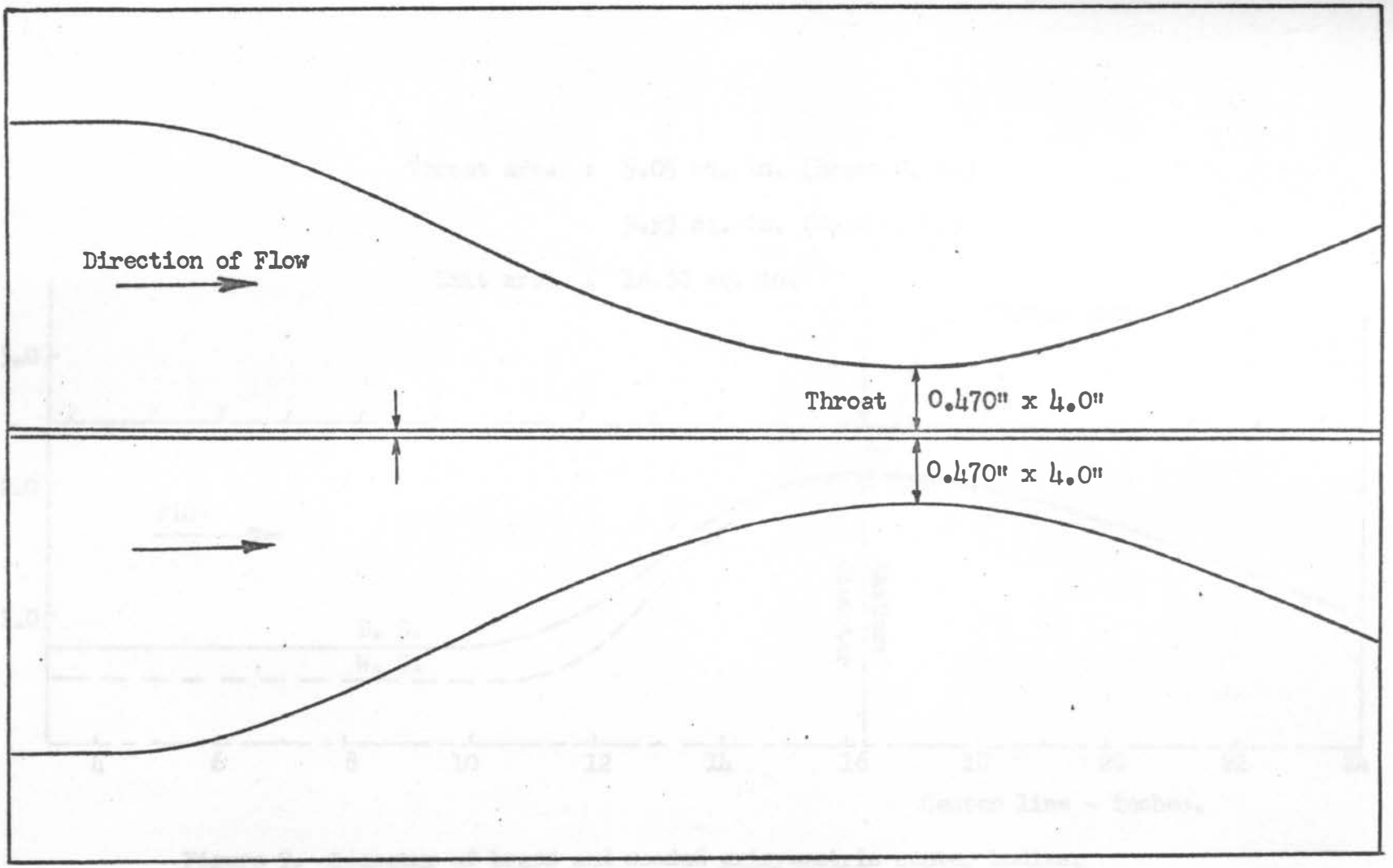

Figure 8. Two-dimensional profile A with dividing plate.

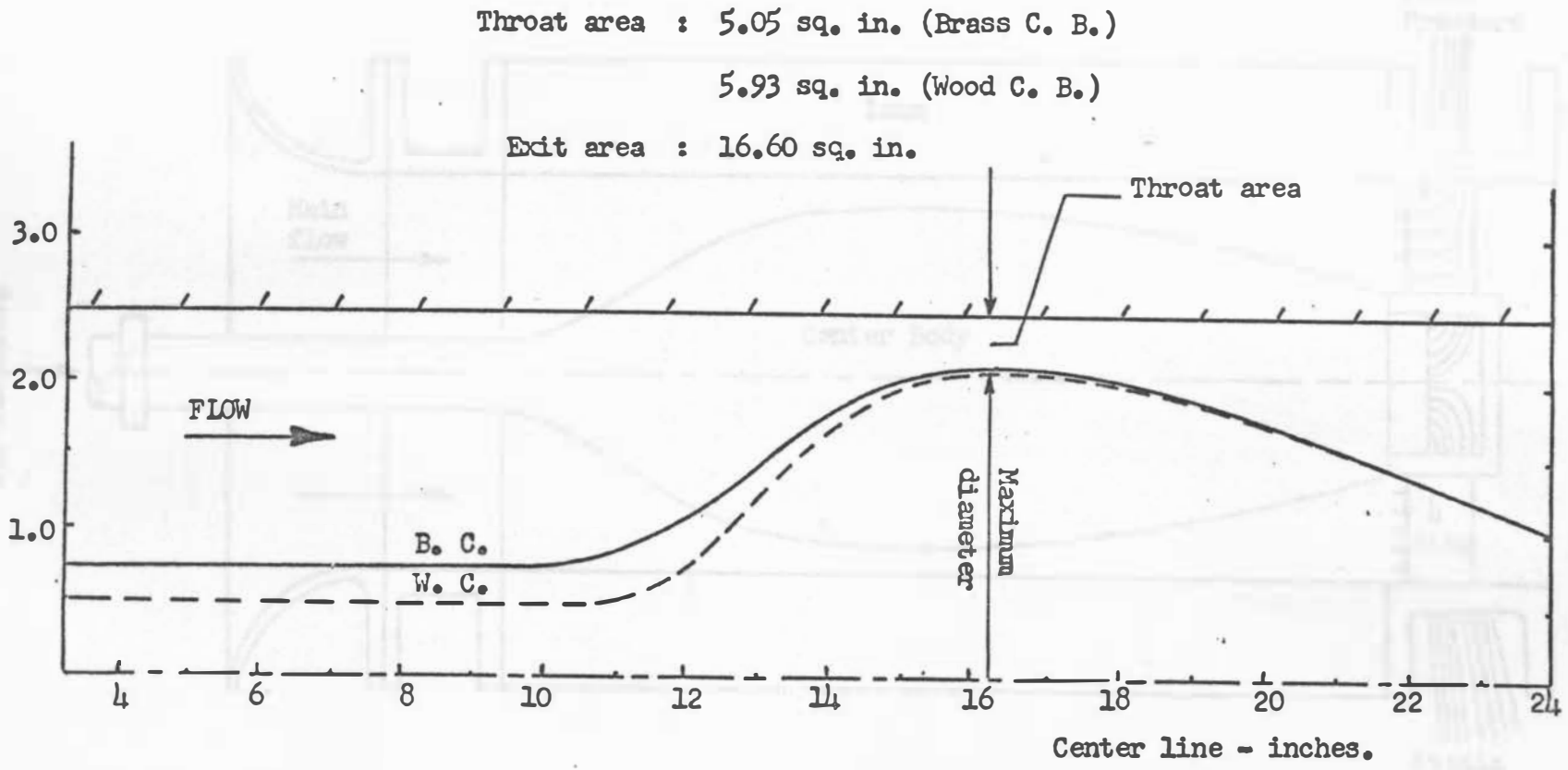

Figure 9. Geometry of brass and wooden axisymmetric center bodies.

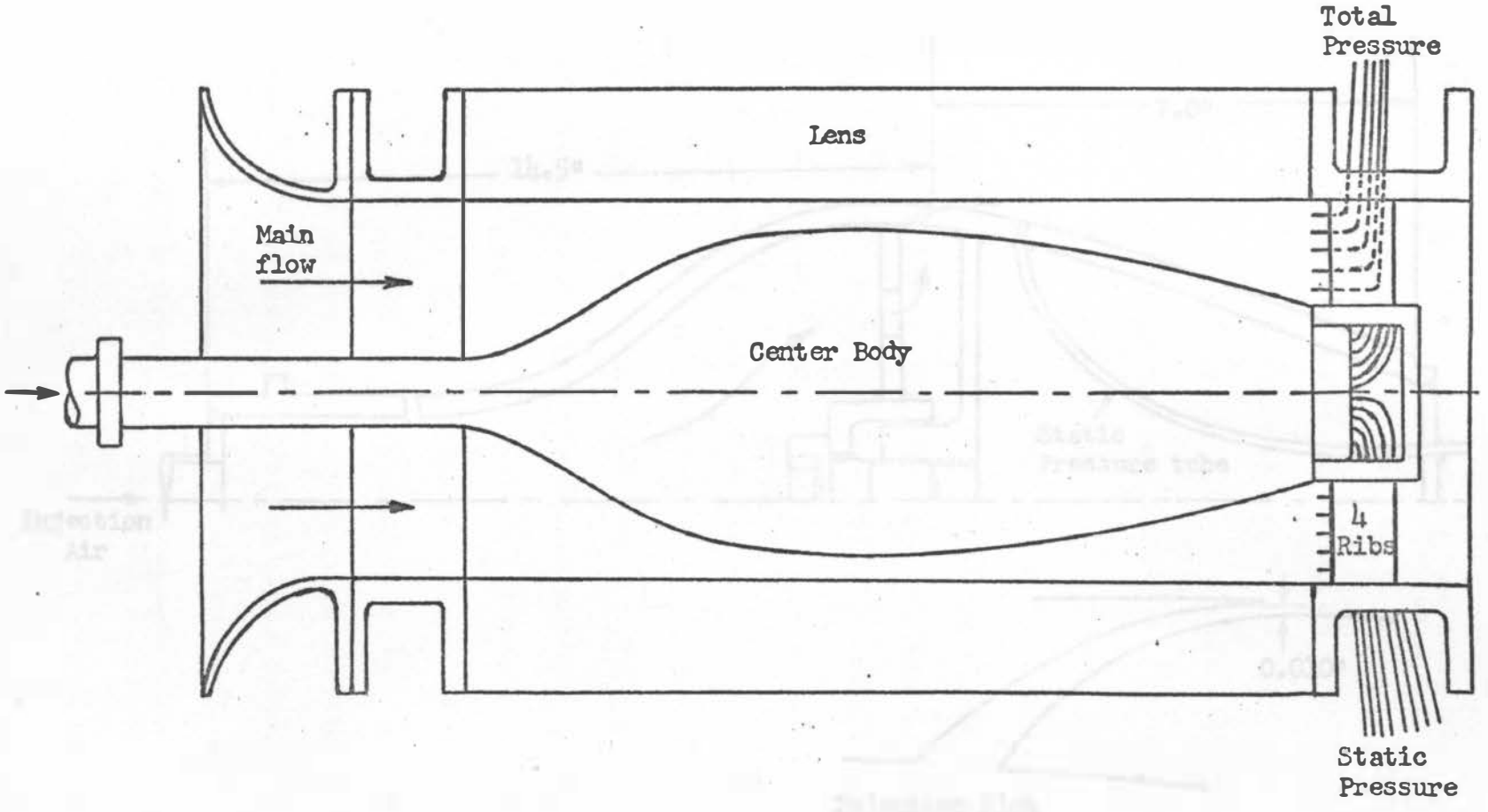

Figure 10. Axisymmetric body assembly.

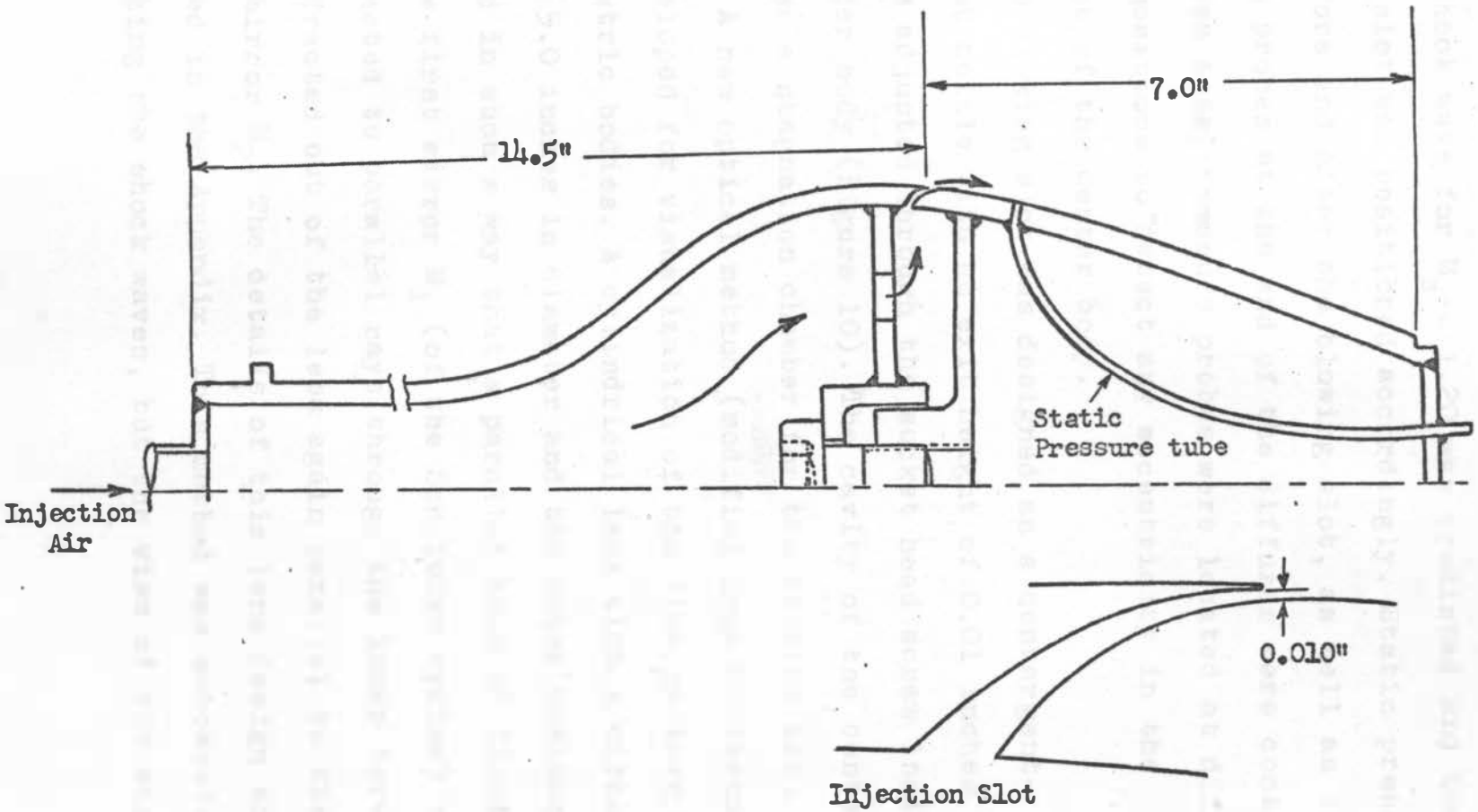

Figure 11. Brass center body.

of the shock wave for M_s = 1.20 was predicted and the blowing slot was positioned accordingly. Static pressure taps before and after the blowing slot, as well as total pressure probes at the end of the diffuser were constructed. These total pressure probes were located at different radial positions to detect any eccentricity in the placement of the center body.

The blowing slot was designed as a convergent-divergent nozzle with an exit height of 0.01 inches which could be adjusted through the socket head screw inside the center body (Figure 10). The cavity of the center body served as a stagnation chamber for the blowing air.

2. A new optical method (modified from Reference 5) was developed for visualization of the flow pattern over axisymmetric bodies. A cylindrical lens with a circular bore of 5.0 inches in diameter and the outer contour designed in such a way that a parallel beam of light coming from the first mirror M_1 (of the Schlieren system) would be refracted to parallel rays through the inner bore and then refracted out of the lens again parallel to the second mirror M_2. The details of this lens design are presented in the Appendix. This method was successful in visualizing the shock waves, but the view of the whole

flow pattern was not very clear, especially away from the center body, as shown in Figure 12. Because of the curvature of the outer contour of the lens, the view on the screen was greatly affected by any deviation of the angle wher the parallel light beam meets the outer surface of the lens. In order to get a better view the parallel beam of light coming into the lens has to be exactly parallel and normal to the flow direction (lens axis) as well as the vertical plane.

3. In order to investigate the nature of the flow along the inner surface of the circular bore of the lens, static pressure measurements were necessary. The lens was then replaced by a plastic tube with the same internal diameter of 5.0 inches and a wall thickness of 0.50 inches.

Figure 12. Shock waves in flow over an axisymmetric body.

CHAPTER IV

ANALYSIS OF TEST RESULTS

A. Two-Dimensional Flow

1. Effect of Upstream Velocity Profile on the Shock Boundary Layer Interaction:

The purpose of these tests using the two-dimensional model is to determine shock stability and the influence of the boundary layer profile upstream of the shock on flow separation. The main shock occurred at an average Mach number of about 1.20 and almost at the same location for all three two-dimensional profiles I, II and III (Figure 13a, b) . The shock strength in all three cases was not very different. Yet, the nature and the shape of the shock wave which occurred in profile I was different than those of profiles II and III. In the case of profiles II and III the main shock had a typical lambda pattern as shown in Figure 13c and also showed an almost constant static pressure region. On the other hand, in case of profile I, a pitot tube was used to measure the boundary layer which made the main shock a normal shock attaching itself to the probe (Figure 13d). At a Mach number of 1.20 ahead of the shock, the flow was quite stable, although

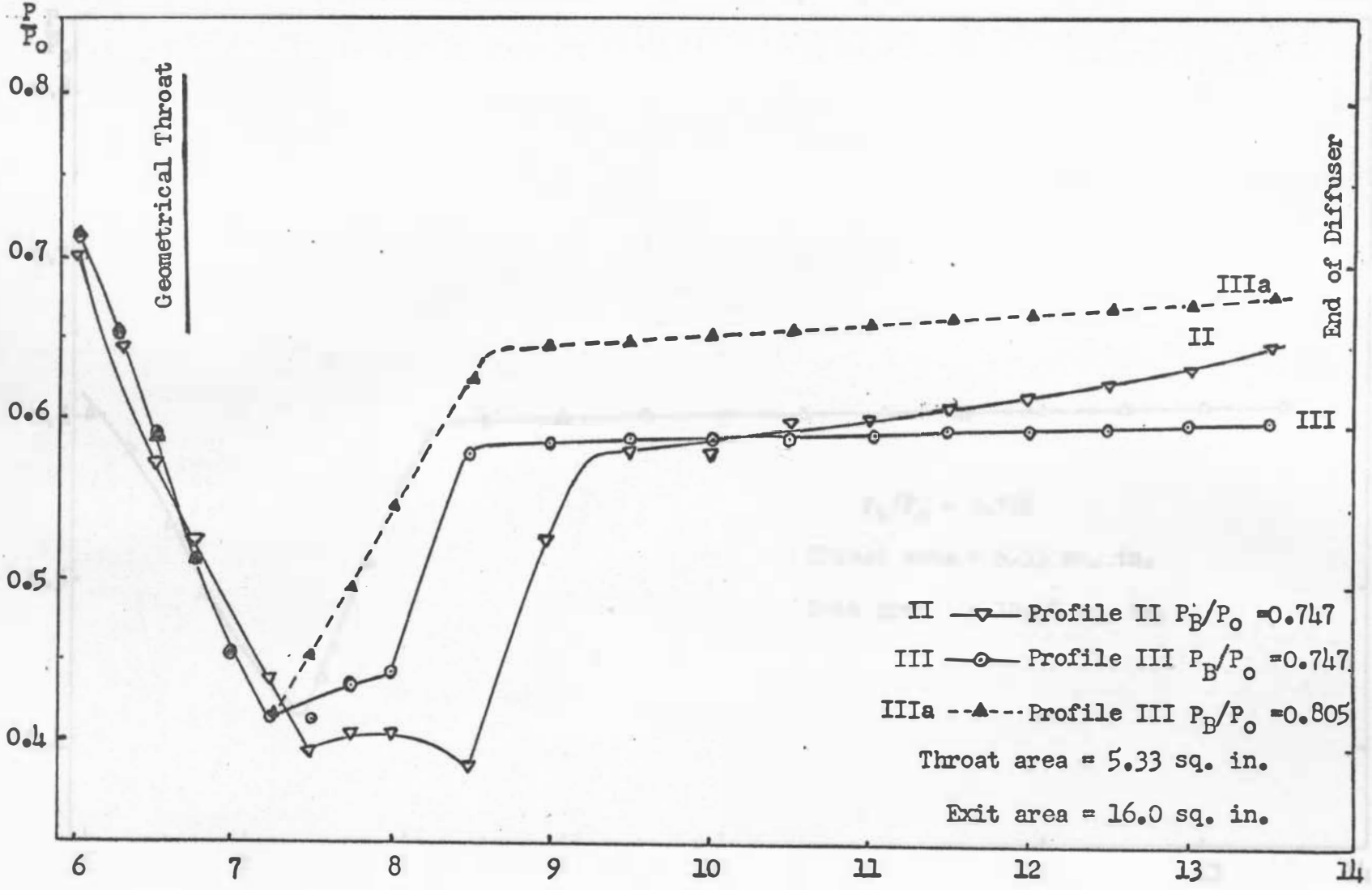

Figure 13a. Two-dimensional profiles II and III.

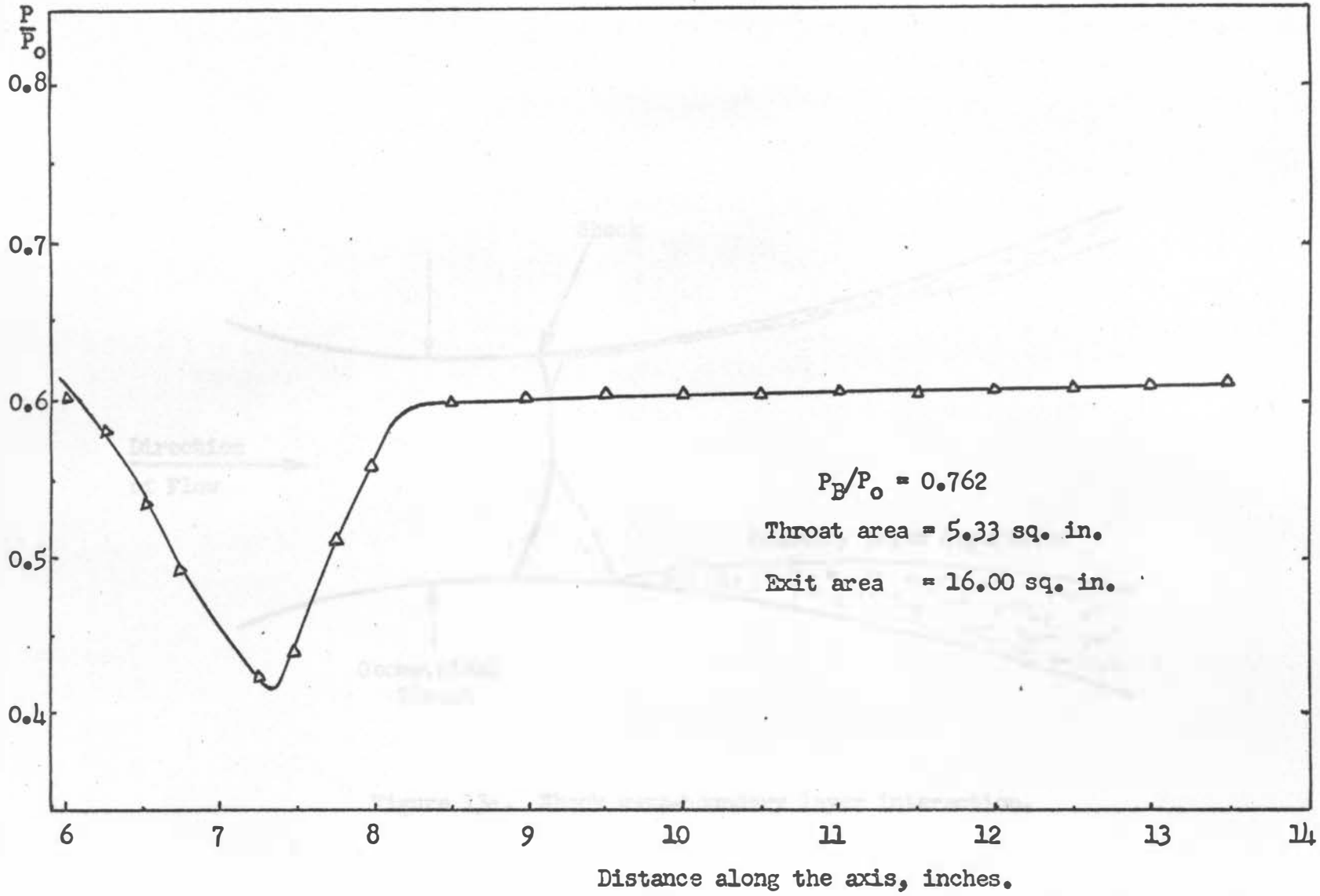

Figure 13b. Two-dimensional profile I.

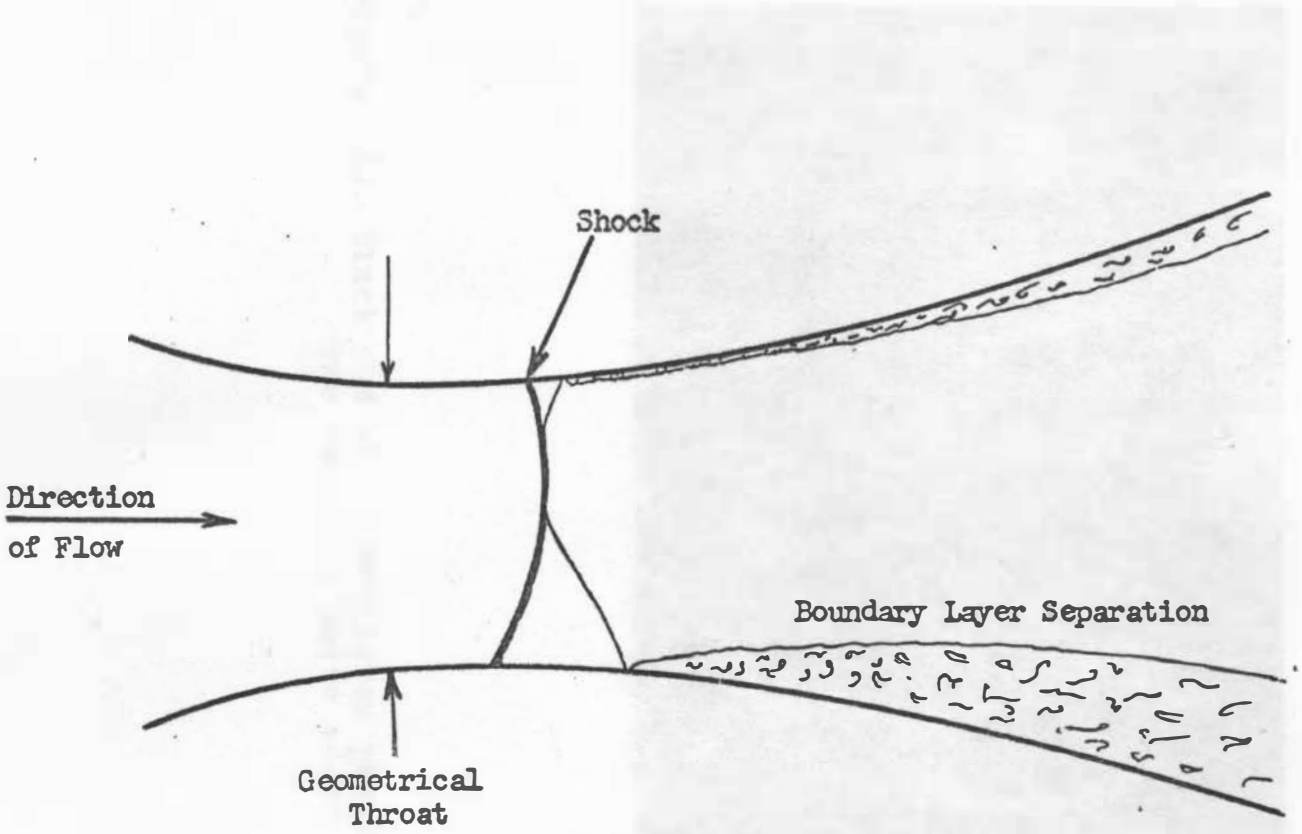

Figure 13c. Shock wave-boundary layer interaction.

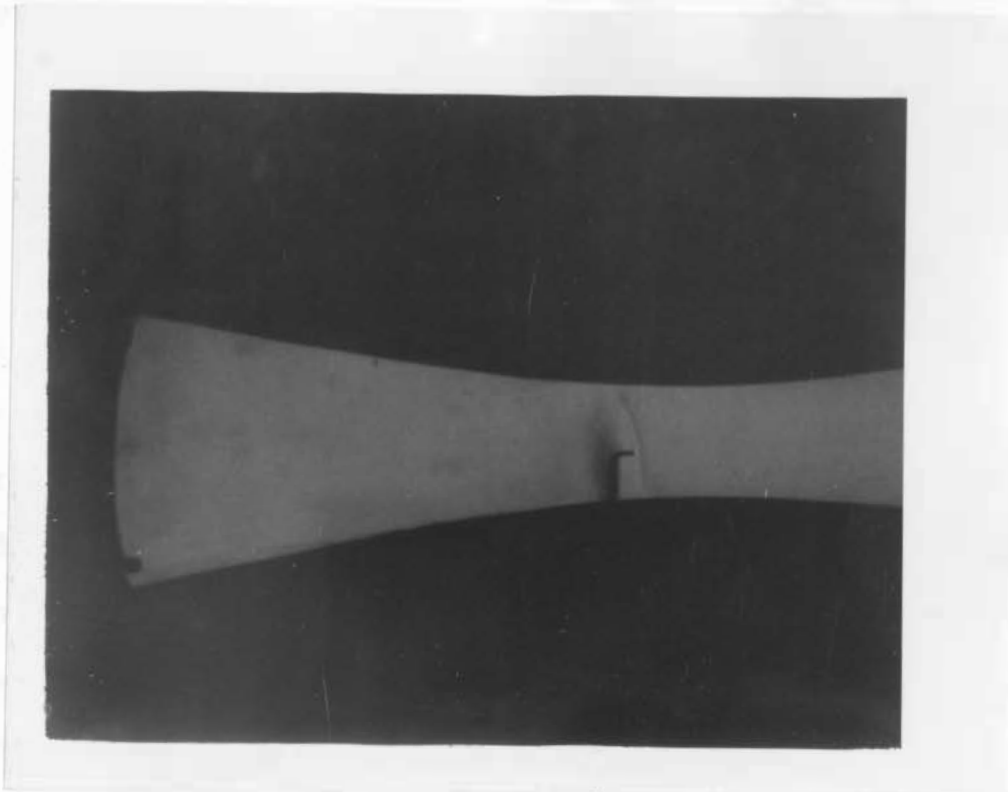

Figure 13d. Black and white Schlieren photo using the vertical knife edge.

severe flow separation occurred on one side of the channel. Curves III and IIIa show the effect of change in back pressure.

2. Suppression of the Induced Flow Separation after a Shock Wave in a Two-Dimensional Convergent-Divergent Nozzle Using a Dividing Thin Plate:

Profile A which is similar to profile I except with a smaller throat area, 4.00 square inches, was tested at a lower back pressure. Curves A1 and A2 of Figure 14 show the pressure distribution on both sides without any dividing plate. The shock wave was not quite normal and occurred at M_s = 1.70 followed by a series of oblique shocks as shown in the photographs of Figure 15. The flow separated very severely off side A2 while the flow remained attached to side A1 (see Figure 15b). This dramatic difference was a result of the relatively high Mach number, and since the flow separated off side A2 the actual channel shape is modified and side A1 remained attached.

The installation of a thin dividing plate accross the convergent-divergent nozzle reduced the throat area of each half to 0.188 square inches and created a normal shock wave in each half ataa higher Mach number (M_s = 1.74),as

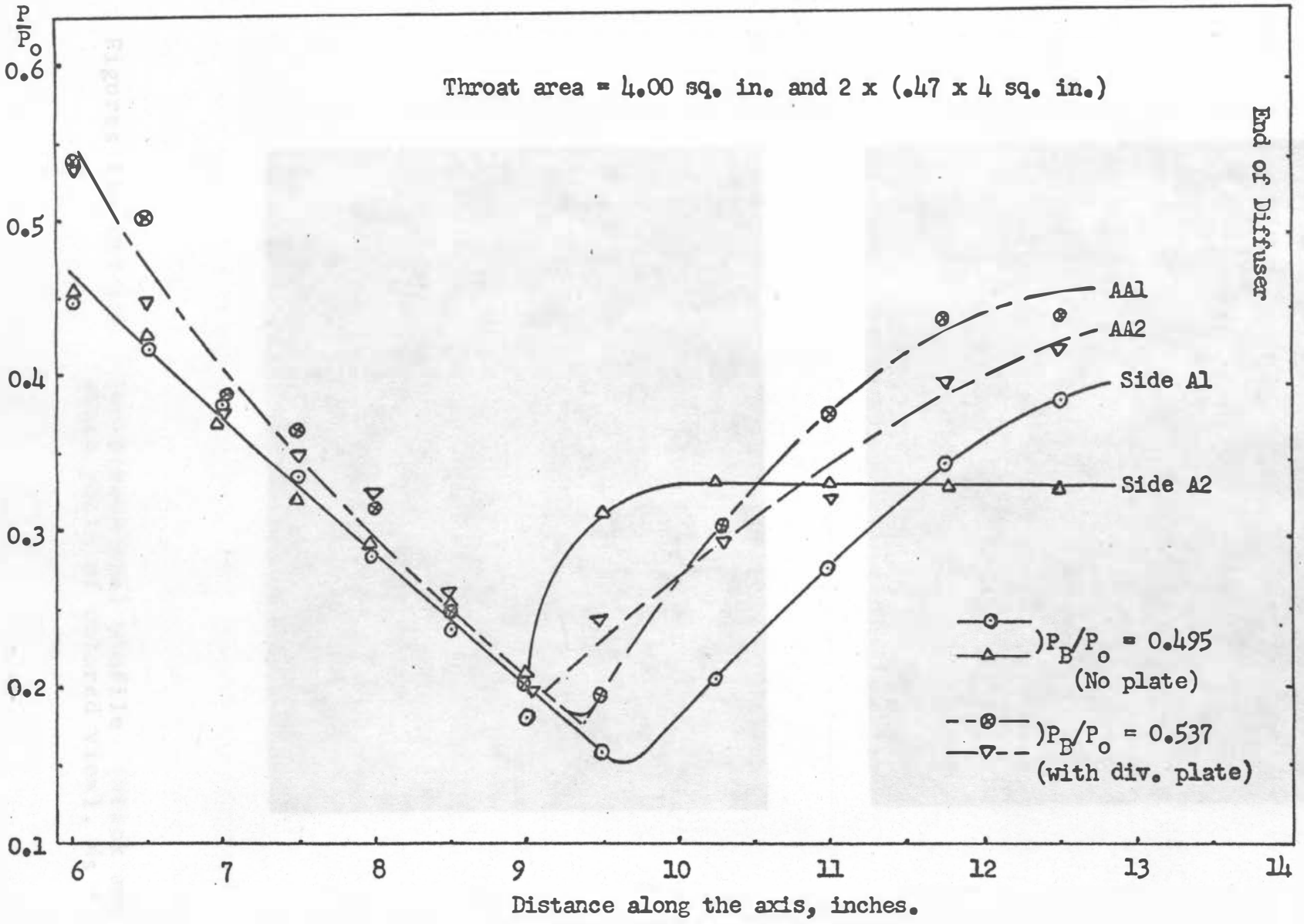

Figure 14. Two-dimensional profile A with and without dividing plate

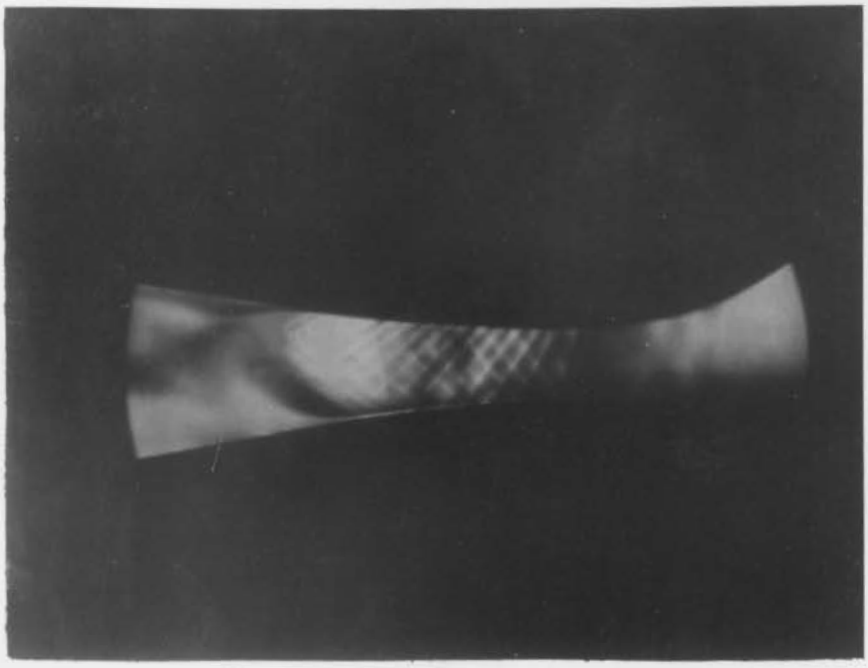

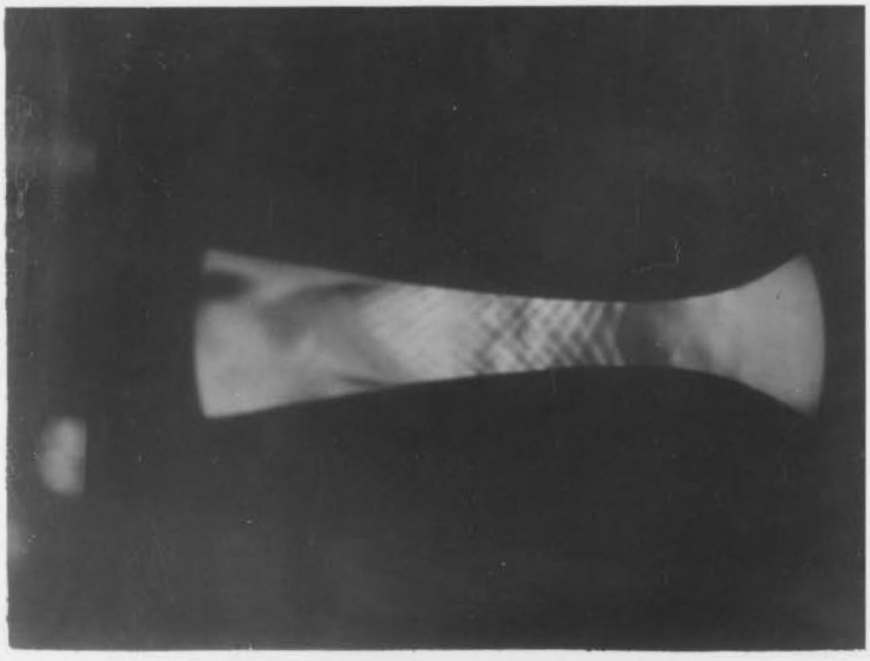

Figures 15a and 15b. Two-dimensional profile (black and white photo of colored view), $M_S = 1.70$

can be seen from curves AA1 and AA2 of Figure 14. Although the shock wave occurred at a higher Mach number, the flow separation off side A2 was suppressed and the flow over the other side (A1) was also improved; only minor separation was noticed. The small difference between the sides as far as the shock location and strength is concerned is merely a result of the accuracy of installing the dividing plate. At Mach numbers 1.32 and lower, the difference was not as noticeable as in the previous case as shown in Figure 16. The Schlieren photographs hardly show any flow separation, which means that by dividing the nozzle into two halves flow separation can be reduced greatly. This is because the rate of diffusion is reduced by $\frac{1}{\sqrt{2}}$ (see Reference 2).

B. Flow Over Axisymmetric Bodies

Two center bodies, a brass center body with an injection slot of 0.01 inches in height and a wooden one with no slot on the surface, were tested at different Mach numbers. They were tested first inside the cylindrical lens to see the flow pattern; then the lens was replaced by the plastic tube with the same internal diameter in order to get the static pressure distribution along the straight wall of the inner bore. The shock waves which occurred in

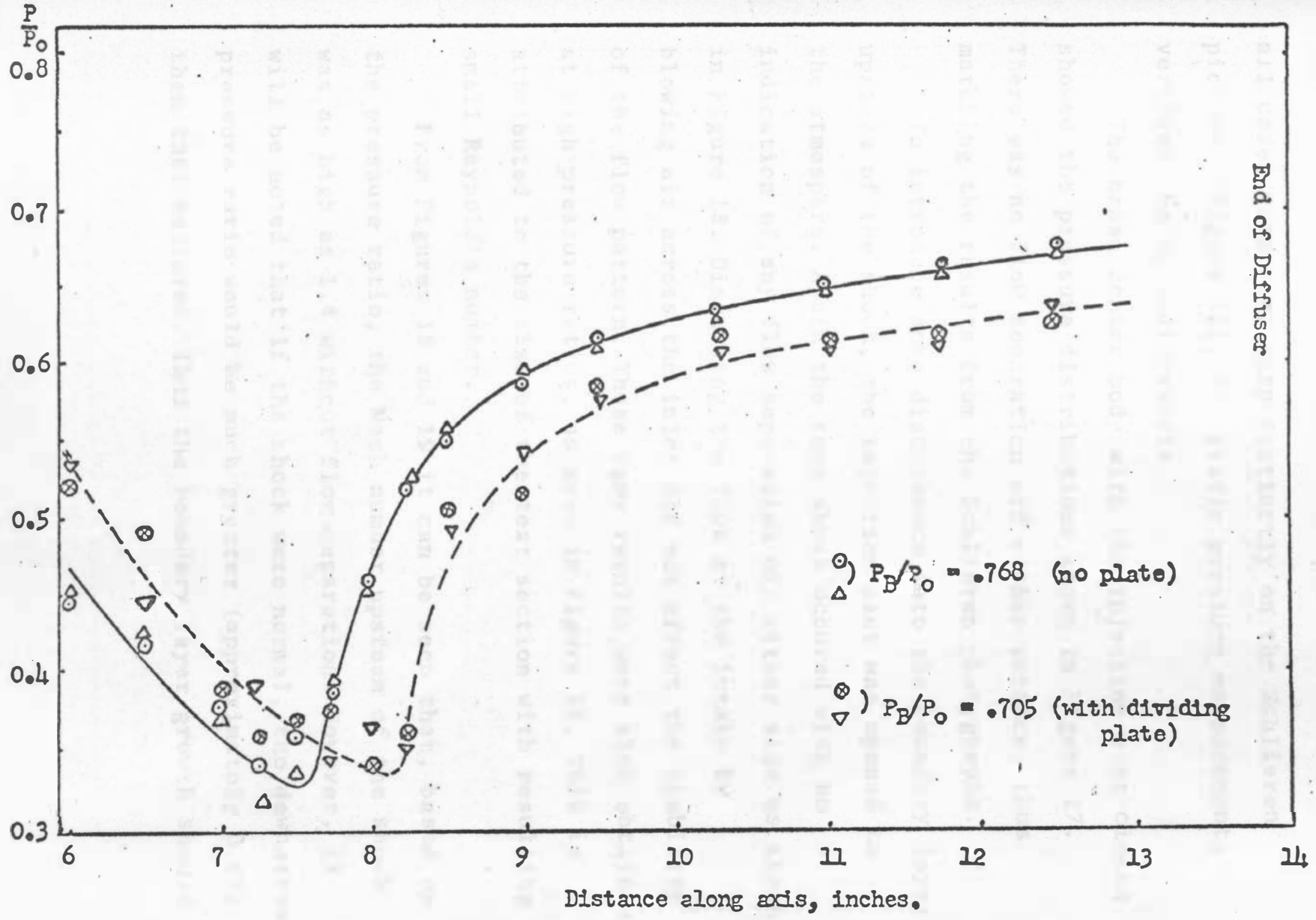

Figure 16. Two-dimensional profile A with and without dividing plate.

all cases were seen very distinctly on the Schlieren pictures (Figure 12). The static pressure measurements verified the optical results.

The brass center body with the injection slot closed showed the pressure distributions shown in Figure 17. There was no flow separation off either surface, thus matching the results from the Schlieren photographs.

To introduce some disturbance into the boundary layer upsteam of the shock, the injection slot was opened to the atmospere. Again the same shock occured with no indication of any flow separation off either side as shown in Figure 18. Disturbing the flow at the intake by blowing air across the inlet did not affect the stability of the flow pattern. These same results were also obtained at high pressure ratios, as seen in Figure 18. This is attributed to the size of the test section with resulting small Reynold's number.

From Figures 18 and 19 it can be seen that, based on the pressure ratio, the Mach number upsteam of the shock was as high as 1.4 without flow separation. However, it will be noted that if the shock were normal, the downstream pressure ratio would be much greater (approximately 0.67) than that measured. Thus the boundary layer growth should

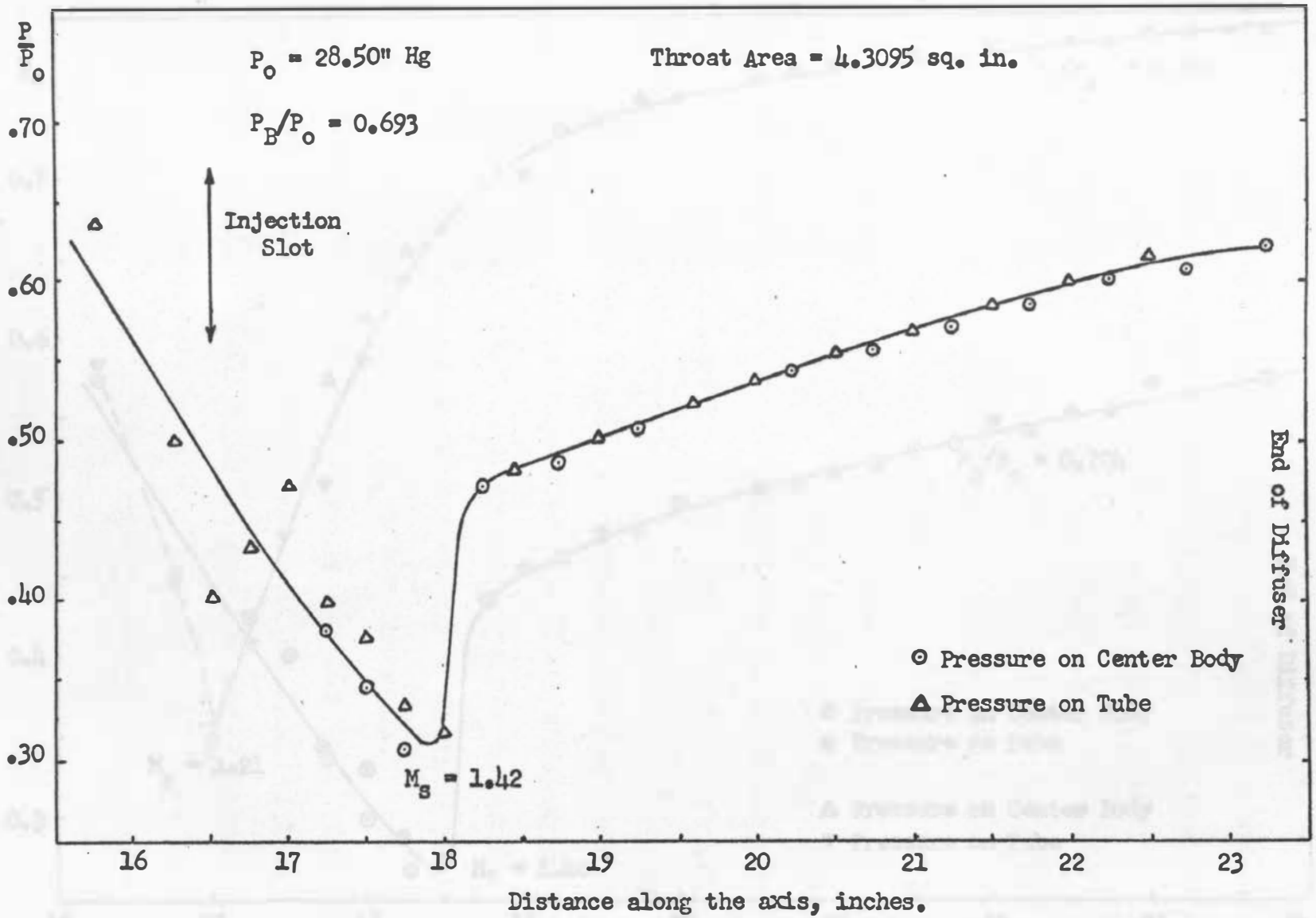

Figure 17. Flow over brass center body: Closed injection slot.

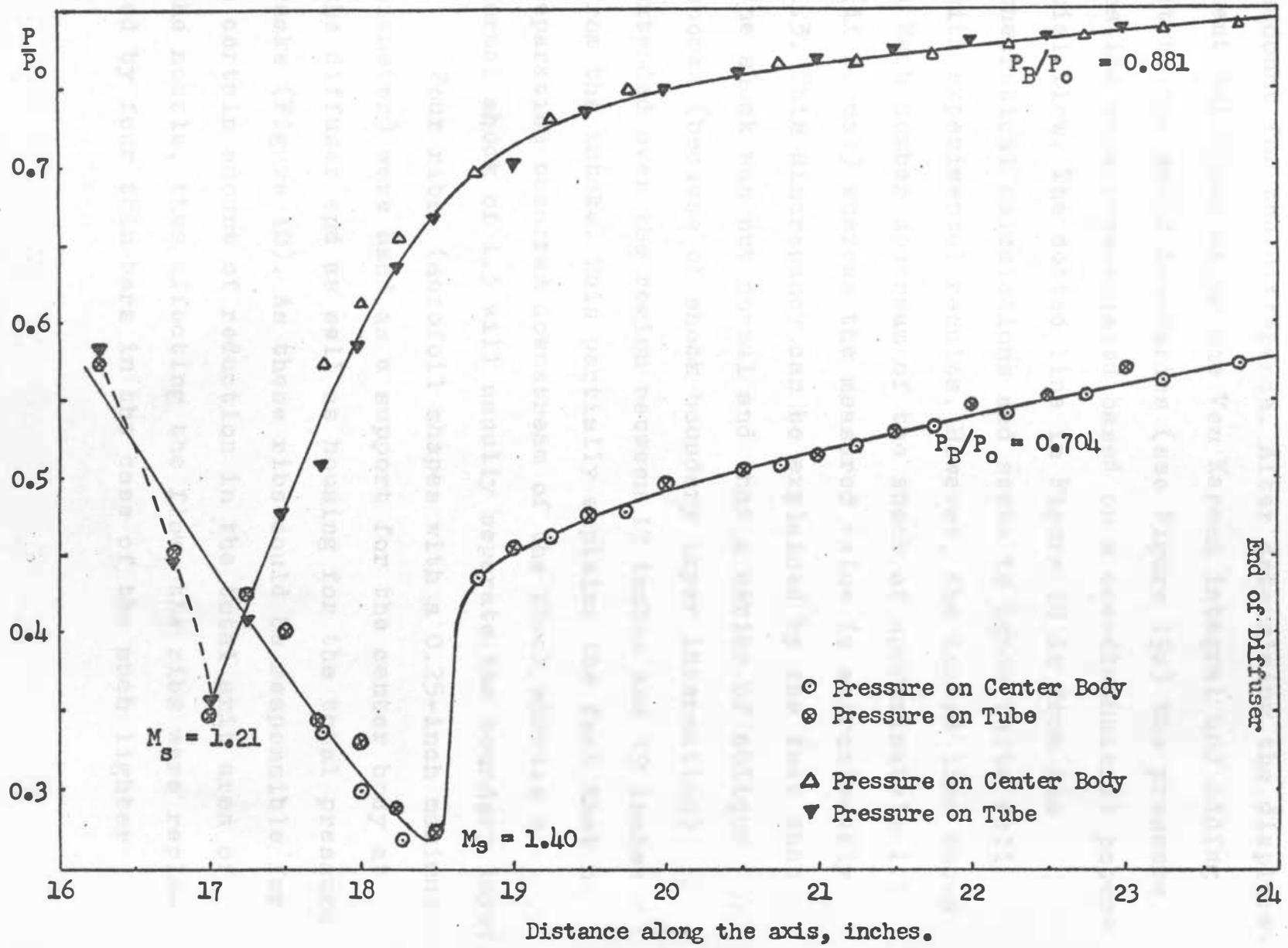

Figure 18. Brass center body: Injection slot open to atmosphere (P_o = 28.50" Hg)

account for the difference. After determining the displacement thickness using the Von Karman integral and adding it to the solid boundaries (see Figure 19a) the pressure ratios were recalculated based on a one-dimensional potential flow. The dotted line in Figure 19 is from the theoretical calculations and seems to agree quite well with experimental results. However, the dotted line shows a Mach number upstream of the shock of approximately 1.1 (if normal) whereas the measured value is approximately 1.3. This discrepancy can be explained by the fact that the shock was not normal and that a series of oblique shocks (because of shock boundary layer interaction) extended over the region between 17 inches and 19 inches from the intake. This partially explains the fact that no separation occurred downstream of the shock whereas a normal shock of 1.3 will usually separate the boundary layer.

Four ribs (aerofoil shapes with a 0.25-inch maximum diameter) were used as a support for the center body at the diffuser end as well as housing for the total pressure racks (Figure 10). As these ribs could be responsible for a certain amount of reduction in the total exit area of the nozzle, thus affecting the flow, the ribs were replaced by four thin bars in the case of the much lighter

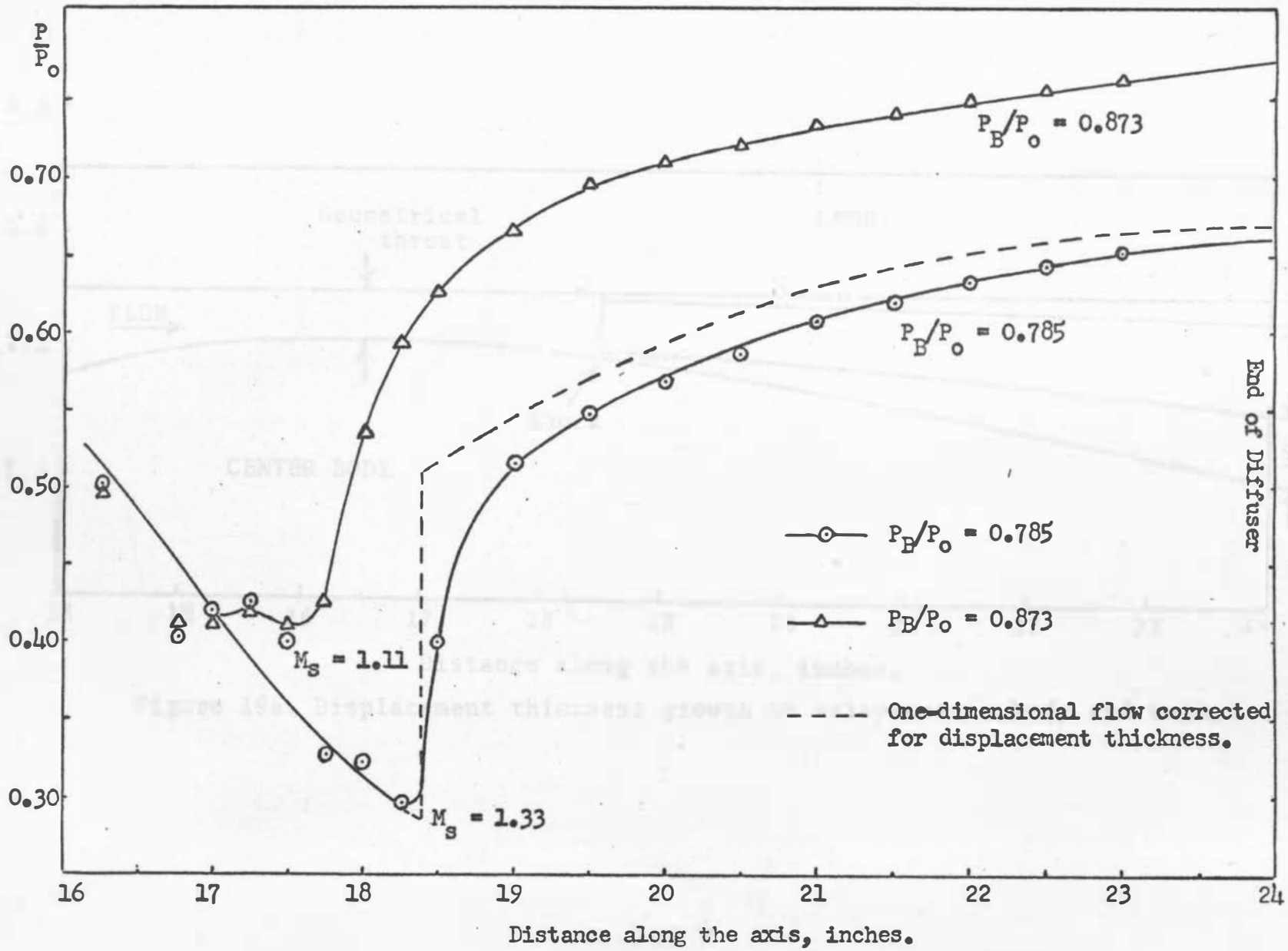

Figure 19. Wooden Center body (total pressure ribs at exit).

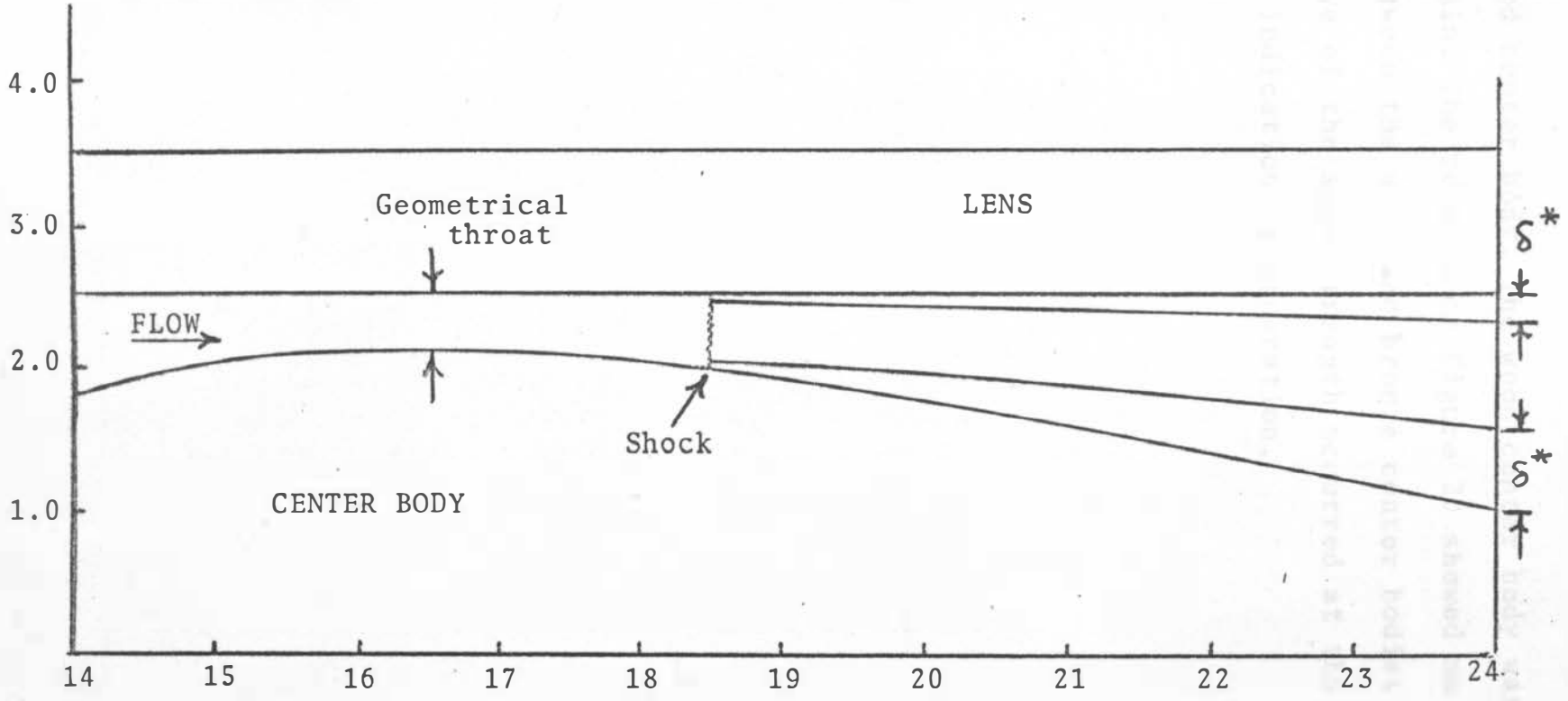

Distance along the axis, inches.

Figure 19a. Displacement thickness growth on axisymmetric body and wall.

wood center body. The wood center body was then tested again. The results in Figure 20 showed no difference between the wood and bronze center bodies. A shock wave of the same strength occurred at the same location with no indication of separation.

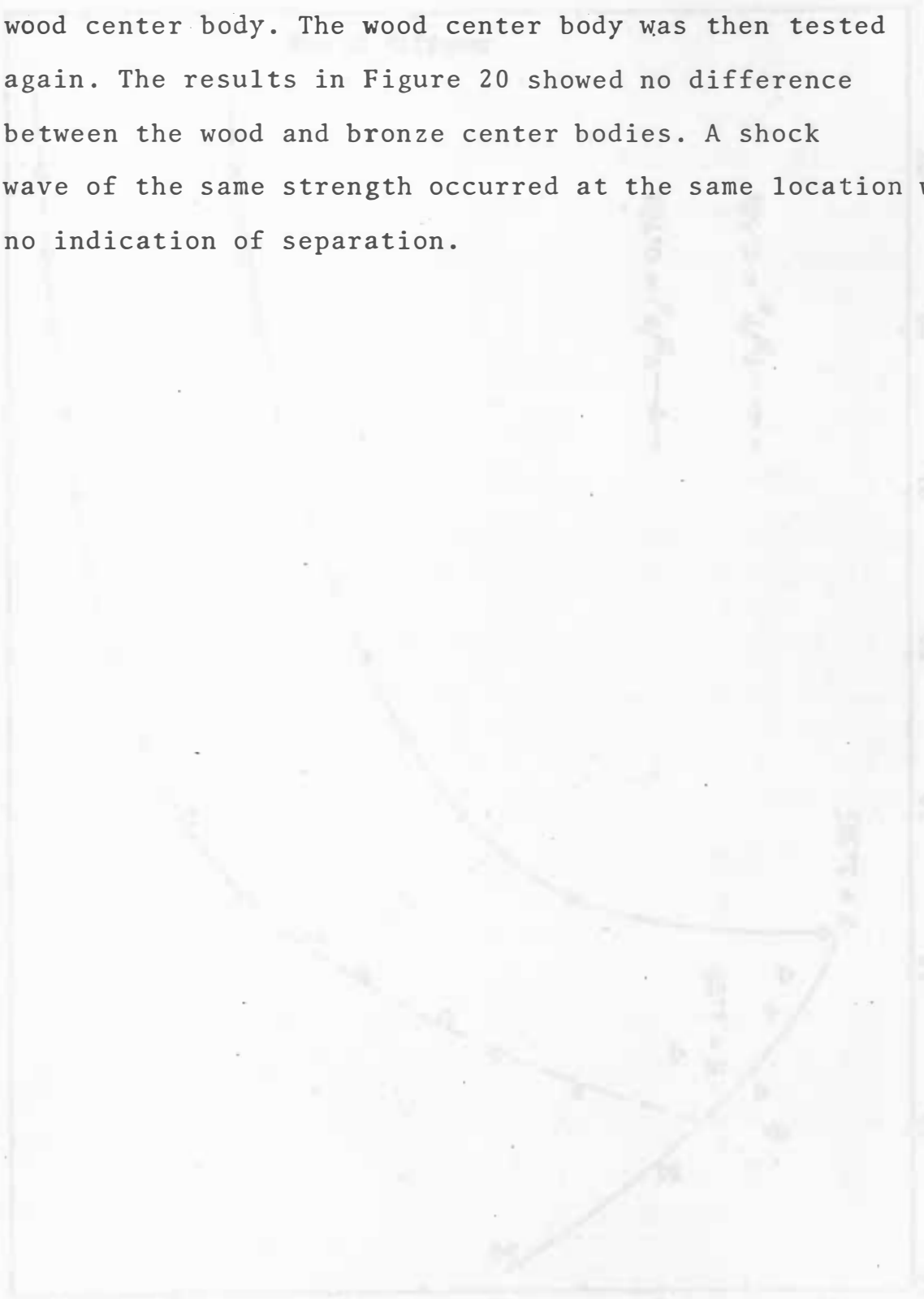

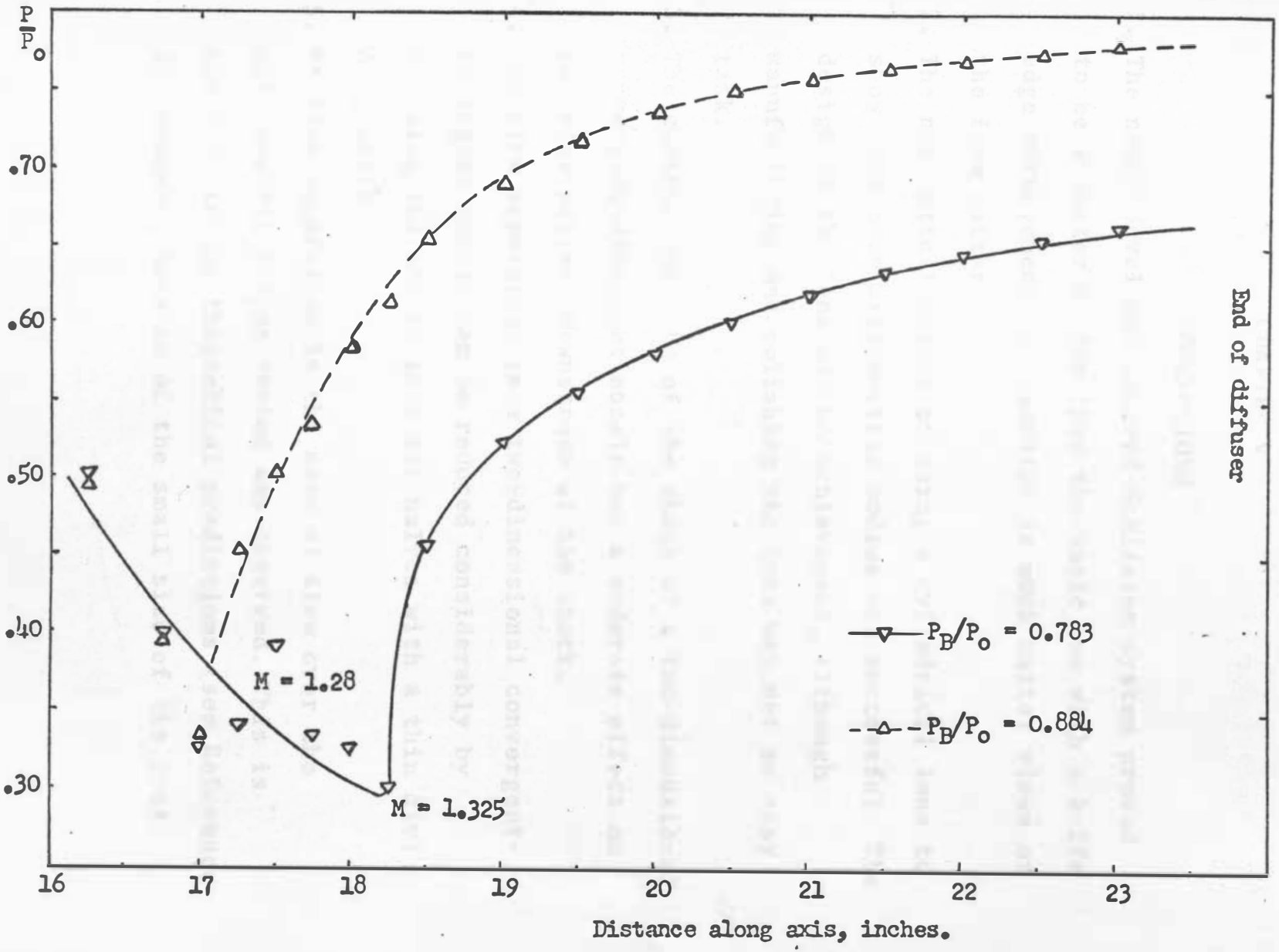

Figure 20. Wooden center body: No ribs at exit area.

CHAPTER V

CONCLUSIONS

1. The newly developed colored Schlieren system proved to be a better system than the basic one with a knife edge arrangement. It resulted in much better views of the flow pattern.
2. The new optical method of using a cylindrical lens to show flow over axisymmetric bodies was successful. The design of the lens was an achievement, although manufacturing and polishing the lens was not an easy task.
3. The contour upstream of the shock of a two-dimensional convergent-divergent nozzle has a moderate effect on the flow pattern downstream of the shock.
4. The flow separation in a two-dimensional convergent-divergent nozzle can be reduced considerably by dividing the nozzle into two halves with a thin dividing plate.
5. No flow separation in the case of flow over the axisymmetric bodies tested was observed. This is contrary to the theoretical predictions (see Reference 2). However, because of the small size of the test

section, reliable conclusions can be drawn only after further tests with a larger facility are made.

CHAPTER VI

RECOMMENDATIONS

Because of the small size of the wind tunnel it is difficult to compare the results with theoretical work (such as that given in Reference 2). In the axisymmetric inlet for example, the height of the throat is only 0.40 inches, and thus it is possible that the flow downstream of the throat is fully developed. Because of the proximity of the upper surface it is less likely for a boundary layer to separate. Thus, though in Reference 2 the theory predicts separation behind the shock, this was not observed in the flow over an axisymmetric body, only in the two-dimensional case. In order to have a good test of the theoretical results of Reference 2, a large test section where the boundary layer and potential flows are clearly defined should be used.

REFERENCES

1. Schlichting, H., Boundary Layer Theory, McGraw-Hill Company, 1968.

2. Lumsdaine, E., and Fathy, A., Theoretical Study of Boundary Layer Control by Blowing for Axisymmetric Flow and its Application to the Sonic Inlet, South Dakota State University Engineering Experiment Station Bulletin No. 16, August 1970.

3. Holder, D. W., North, R. J., and Wood, G.P., Optical Methods for Examining the Flow in High Speed Wind Tunnels, Part I (Schlieren Methods) and Part II (Interferometer Methods), NATO Advisory Group for Aeronautical Research and Development, Paris November 1956.

4. Holder, D. W., and North, R. J., Schlieren Methods, Notes on Applied Science No. 31, London, Her Majesty's Stationary Office, 1963.

5. Jennings, D. R., An Experimental Method for Investigating Three-Dimensional Shock Waves, Sc. D. Dissertation, New Mexico State University, 1965.

6. Shapiro, A. H., The Dynamics and Thermodynamics of Compressible Fluid Flow, Vol.I and II, The Ronald Press Company, New York, 1953.

APPENDIX

Optical Method for Visualization of Flow over Axisymmetric Bodies

The basic principle of the Schlieren system is that a parallel beam of light passing through the test section remains parallel as long as the flow path has a uniform density distribution. So, the lens has to be designed in such a way that with uniform flow inside its bore, a parallel beam of light coming from one side will be refracted parallel inside and comes out parallel from the other side (Figure A-1).

The ray of light at the centerline of the lens meets the lens surfaces at right angles; it does not suffer any refraction by passing through the lens. For the rest of the parallel rays coming to the lens, to come out parallel each of these rays should take the same time to go through the lens as the center ray. Therefore

$$a + uz_o = a + z_o - z \cos(\phi - \theta) + uz \qquad \text{(A-1)}$$

where u is the refractive index of the lens material. Rearranging equation (A-1) so that the coordinates of

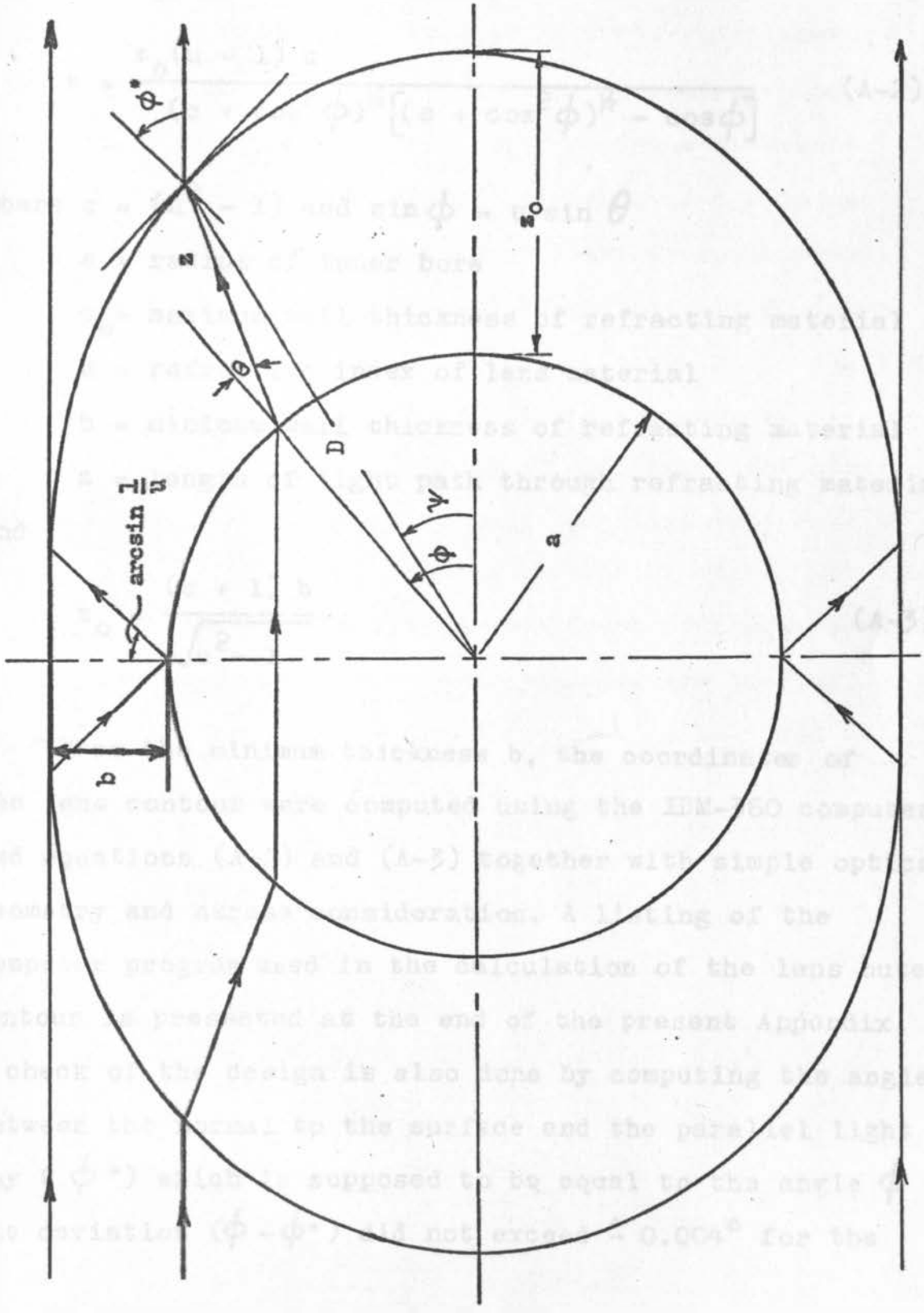

Figure A-1. Cylindrical lens parameters.

the lens can be computed, we get the following relations:

$$z = \frac{z_o(u - 1)\, u}{(c + \cos^2\phi)^{1/2}\left[(c + \cos^2\phi)^{1/2} - \cos\phi\right]} \qquad \text{(A-2)}$$

where $c = (u^2 - 1)$ and $\sin\phi = u \sin\theta$

a = radius of inner bore

z_o = maximum wall thickness of refracting material

u = refractive index of lens material

b = minimum wall thickness of refracting material

z = length of light path through refracting material

and

$$z_o = \frac{(u + 1)\, b}{\sqrt{u^2 - 1}} \qquad \text{(A-3)}$$

From the minimum thickness b, the coordinates of the lens contour were computed using the IBM-360 computer and equations (A-2) and (A-3) together with simple optics geometry and stress consideration. A listing of the computer program used in the calculation of the lens outer contour is presented at the end of the present Appendix. A check of the design is also done by computing the angle between the normal to the surface and the parallel light ray (ϕ^*) which is supposed to be equal to the angle ϕ . The deviation ($\phi - \phi^*$) did not exceed $\pm$ 0.004° for the

range of 0.5 to 15 degrees and was no more than ± 0.0035° in the range over 15 degrees. This check seems to be rather satisfactory. With these coordinates the lens was machined and polished with a linear tolerance of ± .001 inches and an angular tolerance of 6 minutes, which is the best that could be obtained from the optical manufacturing firms. The most critical part for polishing was the section where the lens contour asymptotically ends with the neutral zone along the y-axis. Because the contour tends to be very flat as it approaches the flat-neutral zone it was very difficult to polish that part by any mechanical tracing polishing machine; the only way possible was by hand polishing with frequent checks such as placing a square grid mesh at one side and looking from the other side untill no distortion in the grid was observed.

```
C       CYLINDERICAL LENS DESIGN
    100 FORMAT  (4F10.5)
    101 FORMAT  (1H1,24HCYLINDERICAL LENS DESIGN)
    102 FORMAT  (1H ,35HMAXIMUM BORE RADIUS,  A.....,
       XF7.4,4H IN.)
    103 FORMAT  (1H ,35HCENTER LINE LENS THICKNESS,   B...,
       XF7.4,4H IN.)
    104 FORMAT  (1H ,35HREFRACTIVE INDEX, U.............,
       XF7.4)
    105 FORMAT  (1H ,35HANGLE INCREMENT, DEC.............,
       XF5.2,5H DEG.,/)
    106 FORMAT  (1H ,3HZO=,F7.4)
    107 FORMAT  (1HO,5H(DEG),5X,7H  Z  ,5X,7H  THEA ,
       17X,7H    D   ,7X,7H  PSI ,5X,7H  Y  ,5X,7H  X  ///)
    109 FORMAT  (1H ,F5.2,6(5X,F8.4))
     51 READ (11,100)  DELT,A,B,U
        WRITE (12,101)
        WRITE (12,102)A
        WRITE (12,103)B
        WRITE (12,104)U
        WRITE (12,105)DELT
        C=U*U-1.
        ZO=B*(U+1.)/SQRT(C)
        WRITE (12,106) ZO
        WRITE (12,107)
        DEG=0.
        ANG=0.
        YT = -0.010
     52 YT = YT & 0.010
        DEC = DELT
      1 ANG = DEG/57.29578
        Z=ZO*(U-1.)*U/(SQRT(C&COS(ANG)**2)*(SQRT(C&COS(ANG)
       X**2)
       1   -COS(ANG)))
        TH=SIN(ANG)/U
        THE=ATAN(TH/SQRT(1.-TH*TH))
        THEA=THE*57.29578
        D=SQRT(A*A&Z*Z+2.*COS(THE)*A*Z)
        AP=A*SIN(THE)/D
        ALPA=ATAN(AP/SQRT(1.-AP*AP))
        PSI=(ANG-THE&ALPA)
        Y=D*SIN (PSI)
        X=D*COS (PSI)
        IF ( Y-(YT&0.0001))  5,5,4
      4 DEG = DEG-DEC
        DEC = DEC/10.0
        GO TO 1
      5 IF (Y-(YT-0.0001))  6,2,2
```

```
 6 DEG = DEG + DEC
   GO TO 1
 2 PSI = PSI*57.29578
   WRITE (12,109) DEG,Z,THEA,D,PSI,Y,X
   IF (DEG - 90.) 52,53,53
53 END
```